AN EVALUATION AND ANALYSIS OF URBAN EXPANSION OF KAMPALA FROM 1995 TO 2015

By

Diane Esaete BenBella

B.Sc., Makerere University, 2012

A thesis
Submitted in Partial Fulfillment of the Requirements for the
Master of Science degree

Department of Geography and Environmental Resources
in the Graduate School
Southern Illinois University Carbondale
May 2016

THESIS APPROVAL

AN EVALUATION AND ANALYSIS OF URBAN EXPANSION OF KAMPALA FROM 1995 TO 2015

By

Diane Esaete BenBella

A Thesis Submitted in Partial

Fulfillment of the Requirements

for the Degree of

Master of Science

in the field of Geography and Environmental resources

Approved by:

Dr. Guangxing Wang, Chair

Dr. Justin Schoof

Dr. Leslie Duram

Graduate School
Southern Illinois University Carbondale
2/29/2016

AN ABSTRACT OF THE THESIS OF

DIANE ESAETE BENBELLA, for the Master of Science degree in GEOGRAPHY AND ENVIRONMENTAL RESOURCES, presented on 2/29/2016, at Southern Illinois University Carbondale

TITLE: AN EVALUATION AND ANALYSIS OF URBAN EXPANSION OF KAMPALA FROM 1995 TO 2015

MAJOR PROFESSOR: Dr. Guangxing Wang

The rapid expansion of urban areas as a result of population growth and economic prosperity is causing land use and land cover (LULC) changes in cities all over the world. Kampala, Uganda, is no exception to this trend. Currently, Kampala's population stands at 1.9 million people, and this number is expected to rise in the next coming years. Consequently, a large population will burden the already fragile ecosystems that characterize the urban landscape. The aim of this study was to derive the spatial patterns of urbanization as well as identify drivers of urbanization in Kampala using geographic information system (GIS) and remote sensing technologies. I used multi-temporal Landsat images (1995, 2010, and 2015) and produced classification maps using Artificial Neural Network (ANN) and Spectral Mixture Analysis (SMA). The results showed that there has been an overall expansion of urban areas at the expense of other LULC types especially in the Northern part of the city. There has been a significant reduction in subsistence agriculture and vegetation. The temporal period between 1995 and 2010 showed the highest conversion of subsistence agriculture and vegetation to urban areas. The overall urban expansion rate from 1995 to 2015 was 3.4 %. Using Markov simulation, I generated a LULC map for the year 2025 that showed a 15 % increase in urban areas. I analyzed various factors that I hypothesized drove urbanization. Population growth was the major driver of urbanization. Economic factors such as Gross Domestic Production (GDP) and Foreign Direct Investments (FDI) also played a significant role in the increment of urban areas in

Kampala. Other factors such as distance to roads, distance to disturbance and policy have also contributed to urban growth. The findings of this study provided decision makers as well as the public with reliable information about LULC changes and the factors influencing these changes.

DEDICATION

To my family who have been my constant source of encouragement and support. Thank you for always believing in me.

ACKNOWLEDGMENTS

First, I would like to thank my advisor Dr. Guangxing Wang for his insight throughout this research. My advisor's knowledge, guidance and patience allowed to me grow in Remote Sensing. I would also like to thank Dr. Justin Schoof and Dr. Leslie Duram for taking the time to read my thesis and giving me great insights from their academic experience. Lastly, I would like to thank my fellow graduate students and friends at the Department of Geography for their contributions to my research and their support and encouragement.

TABLE OF CONTENTS

LIST OF TABLES

TABLE PAGE

LIST OF FIGURES

FIGURE PAGE

CHAPTER 1

INTRODUCTION

According to the United Nations (UN, 2014), the world is experiencing urban growth at an unprecedented rate. Nearly half of the world's population resides in cities. This number is expected to increase to 69.6 % in the next 30 years (Yuanbin et al., 2012). Urban growth is often correlated with economic growth and is considered a sign of economic vitality (Yuan et al., 2005). Ade and Alofabi (2013) noted that urban areas are monopolies of innovation, employment, and production attracting people to them. Consequently, large urban populations are putting a strain on the already fragile urban ecosystems resulting in environmental degradation, land fragmentation, and loss of ecosystems and ecosystem services.

The urban population in most African countries is increasing faster than anywhere else in the world with over 60% of the total population living in the central cities (Mubea et al., 2012).Population growth is attributed to the fast-growing economies that are characterizing the continent (IMF,2012). Most cities in this region are poorly planned, and increased urbanization due to population growth further aggravates the situation. Rapid population growth has had a substantial effect on the growing demand for social services, infrastructure, housing, energy, water that has ultimately negatively affected the way land is being used.

Kampala, Uganda's capital city, is no exception to this trend with 1.9 million out of its 35 million population being permanent residents. This number is expected to double in the next ten years (World Bank, 2013).Kampala has undergone significant land use and land cover (LULC) changes as a result of urbanization. The process of urbanization has mainly been typified by population growth, infrastructure development, and increased use of land resources. Lack of adequate land use planning by the Ministry of Finance, Planning and Economic development of

Uganda has resulted in urban sprawling. Urban sprawling is the uncontrolled physical expansion of built-up areas at the expense of other LULC types. It is, therefore, important to quantify patterns of LULC changes in Kampala to mitigate some of these consequences and to plan for the city better.

1.1 Research Purpose

The purpose of my study is to derive the spatial patterns of LULC types and their dynamics for Kampala over the last 20 years using remote sensing and GIS technologies. This study seeks to determine how urbanization has contributed to LULC changes in Kampala and how population increase as well as other factors such as distance to roads, distance to disturbance, foreign investments, and GDP per capita have contributed to urbanization. Using Markov model, this study will further predict how LULC will change in Kampala in the next ten years. Ultimately, findings of this study are intended to form the basis for a better understanding of the dynamics of LULC processes in urban areas. This study will be beneficial to researchers and policy makers as they establish sustainable development strategies.

1.2 Research Questions

Hypothesis

There has been an increase in urbanization at the expense of other LULC classes such as vegetation and subsistence agriculture. The increment in urbanization is a direct consequence of the increased urban population and other variables that will be determined during this study.

In this study, the above hypothesis will be tested and at the same time, the following questions will be answered:

1. What are the spatial and temporal patterns of LULC changes in Kampala over the last 20 years?

2. How has urbanization driven these changes of LULC types?

3. What are the major drivers of urbanization?

1.3 Significance of Study

- There have been few studies about LULC changes of Kampala using geospatial technologies such as remote sensing and GIS. This study will provide a baseline for other studies in Kampala using geospatial technologies.

- It will provide information necessary for urban and environment planning and monitoring that is of benefit to the different ministries in charge or urban development and the environment. It will also provide the framework for policy about urban expansion.

- It will also open up the possibility of using geospatial tools for environmentalists, regional and urban planners for monitoring and planning urban environment in Uganda.

1.4 Limitations

There will be no field work verification on my part. My work will purely be using satellite images and validated by 2010 and 2014 aerial photographs.

CHAPTER 2

LITERATURE REVIEW

2.1 Land use and Land cover

Understanding the dynamics of LULC change is very significant because of its environmental impacts (Fan et al., 2007; Wondrade et al., 2014). These environmental impacts include loss of biodiversity, soils and their fertility, water quality, and air quality. Based on Reid et al. (2000), land use activities contributed to greenhouse gas emission by 55 %. Proximate and Underlying factors influence LULC change. Proximate causes explain how the land cover is influenced directly by human activities, for example, agricultural expansion or infrastructure development, and operate at a local level (individual farms, households). On the other hand, underlying causes operate at global and regional scales and are the motives for the proximate causes and are often exogenous. Underlying causes tend to be more complicated as a result of interactions among social, political, economic, demographic, technological, cultural, and biophysical variables. (Lambin, 1997; Lambin and Geist, 2007).

2.2 Main drivers of LULC Changes

The primary drivers of LULC changes mainly include:

Natural variability: Natural environmental changes interact with human decision-making processes, causing LULC changes. Highly variable ecosystem conditions driven by climatic variation amplify the pressures arising from high demands on land resources, especially under resource-limiting conditions (Lambin et al., 1997; Lambin and Geist, 2007).

Technological and economic factors: Mechanization of agriculture as a result of technological advances has increased the intensity of crop and animal production. Consequently, more forest lands and wetlands are being cleared for large-scale agriculture and this has altered the LULC of that area. Incorporating technology into agriculture is usually an indicator of the economic vitality of a society. Farmers with a higher standard of living tend to incorporate the use of intense technologies into their farming (Lambin et al., 1997; Lambin and Geist, 2007).

Demographic factors: Population increase in a particular region often speeds up LULC changes. Cities provide an environment in which people have higher incomes and more job opportunities, inducing a migration of people from rural areas into cities (Wu et al., 2006).

Institutional factors: LULC changes are influenced directly by political, legal, economic, and traditional institutions and their interactions with individual decision making. Local and national policies often determine access to land, labor, capital, technology and information. Land degradation and other negative environmental consequences of LULC changes are often the results of ill-defined policies and weak institutional enforcement that undermine local adaptation strategies. On the other hand, the recovery or restoration of land is also possible with appropriate policies (Lambin et al., 1997; Lambin and Geist, 2007).

Cultural factors: The motivations, personal histories, attitudes, beliefs, and individual perceptions of land managers influence land use decisions (Lambin et al., 1997; Lambin and Geist, 2007). For example, early cultural beliefs in Africa ensured the preservation of individual LULC types. Before the coming of Christianity and Islam, many perceived nature as a sacred and holy place where the gods of the African traditional religion dwelled. As a result, nature was left intact as a sign of respect. However with the changing mentality of Africa's youth, the sacred

views of certain LULC types are no longer held. As a result, forested land is being cleared to meet the growing demands of the population.

Globalization: Globalization processes can amplify or reduce driving forces of LULC change.These processes remove regional barriers and weaken national connections, as well as increase the interdependency among people (Lambin et al., 1997; Lambin and Geist, 2007). Globalization is a good example of the underlying cause of LULC changes. It is involved in technological factors, demographic factors, institutional and cultural factors (Lambin et al., 1997; Lambin and Geist, 2007).

2.3 Urbanization

In western nations such as USA, Britain and France, the urbanization process in the 18th and 19th centuries was fueled by the industrial revolution (Ade and Afolabi, 2013). Furthermore, the Dust Bowl in the USA in the 1930s drove 60% of the population of the Great Plains region out of this region to California and other states that were not affected by the dust storms. The Dust Bowl resulted from poor farming practices, weather and drought that rendered most top soils loose and as a result could be easily carried by strong winds. However, in sub-Saharan Africa, urbanization is mainly linked to population increase resulting from high birth rates and migrations from rural areas (Ade and Alofabi, 2013). Migration is the long-term relocation of individual households or groups domestically or internationally and is influenced by either "push factors" or "pull factors". Push factors are perceived by migrants as detrimental causing a departure of people from that area. These factors include war, disease outbreaks, and natural disasters. Pull factors are opportunities for personal development attracting high numbers of individuals to move to that area or region (Ade and Alofabi, 2013). Socio-economic policies

drive urbanization. Cities such as Beijing and Shanghai in China emerged due to the economic reform in 1978 (Wu et al., 2006). Other factors such as traffic conditions, good infrastructure, distance to roads and urban centers, presence of excellent medical facilities have contributed to urbanization (Xiao et al., 2005; Wu et al., 2006; Mohan et al.,2011)

In Uganda, urbanization has resulted from the political stability that was ushered in by the new government in 1986 after years of military coups and civil wars. Consequently, the shattered infrastructure and economy was rebuilt. The government set up the policies that encouraged foreign companies to invest in the country and the set-up of small businesses

Population increase naturally creates adjustment and readjustment of human land use activities, thus causing an area to undergo lateral and structural changes (Ade and Afolabi, 2013). If well managed, urban areas offer extraordinary opportunities for economic and social development. Urban areas are a focal point for economic growth, innovation, employment and production (Cohen, 2006).

However, uncontrolled urbanization leads to urban sprawling (Mundia and Aniya, 2006) Urban sprawling results in open space creation, loss of forested and fertile agricultural lands, fragmentation, degradation, and isolation of natural areas. The corresponding results are a decline in natural vegetation cover, climate change at local, regional and global scales, and disappearance of ecologically sensitive habitats in and around urban areas. Since anthropogenic activities strongly influence ecosystems in urban areas, more attention should be directed towards monitoring their changes (Mohan et al., 2011). Uncontrolled urbanization also results in increased pollution that has adverse effects on human health, the development of urban poverty, and the rise of slums. As estimated, about 72 percent of the urban population in Africa now lives

in slums. This proportion is about 43 percent in Asia and the Pacific, 32 percent in Latin America, and 30 percent in the Middle East and Northern Africa (Cohen, 2006).

2.4 LULC change Detection

Remote sensing and GIS have made it possible to study LULC changes over different time periods (Weng, 2002). During the last several decades, various remote sensing methodologies have been applied to different studies to understand the dynamics of LULC with great success. However, LULC changes are often over-estimated, and thus, improvements in these technologies are necessary to increase accuracy (Li and Yeh, 2004).

2.4.1 Imagery

LULC information is extracted from remote sensing imagery obtained from both passive and active remote sensors. There are three types of imagery obtained from passive remote sensors namely coarse, medium and high spatial resolution imagery. Coarse spatial resolution images such as Advanced Very High Resolution Radiometer (AVHRR) and Moderate-resolution Imaging Spectroradiometer (MODIS) have been widely employed to detect LULC changes at global and regional scales (Vogelmann et al., 2001). Lambin et al. (1997) used AVHRR to identify LULC changes that had taken place in sub-Saharan Africa. Dubovyk et al. (2012) used the widely available MODIS data to analyze the spatial and temporal patterns of cropland degradation in the irrigated lowlands of Uzbekistan. Coarse spatial resolution images can be downloaded at no cost, however; coarse spatial resolution data limits the provision of spatially detailed information of LULC changes (Vogelmann et al., 2001).

Medium spatial resolution imagery, such as Landsat and SPOT, is the most commonly used imagery when it comes to LULC (Vogelmann et al., 2001). Landsat images are freely available and provide a 30 m by 30 m imagery every 16 days. Landsat images have been utilized effectively in various regional to national scale LULC change investigations such as ecosystem health, land cover assessment, and other land management issues. (Vogelmann et al., 2001). Mundia and Aniya (2006) used Landsat imagery to analyze the dynamics of LULC change and degradation of Nairobi City, Kenya. Yuanbin et al. (2012) utilized Landsat TM/ETM+ imagery to monitor Urban Expansion and its influencing factors in the Natural Wetland Distribution Area in Fuzhou City, China. SPOT imagery, on the other hand, is not freely available, and this makes it unsuitable for large-scale LULC studies. However, it has been widely successful in mapping homogenous landscapes and classification of urban and industrial areas. SPOT captures spectral information at a 2.5 to 20-meter resolution (Li and Yeh, 2004). Keller and Lamprecht (1995) used SPOT in their research about road dust being an indicator of air pollution. They required a multi- spectral sensor that had to be sensitive enough to discern dust and vegetation in both the visible and near-infrared radiation spectrum.

In addition to satellite remotely sensed data, aerial photographs are often utilized to detect LULC changes in a given temporal period. Aerial photographs are fairly inexpensive and provide spatial and temporal information for local scale LULC investigation (Jensen and Cowen, 1999). Mendoza et al. (2002) utilized standard black and white aerial photographs for their study of Multi-temporal analysis of land cover changes in Colombia and generated ecological maps to be used in LULC change detection. However, aerial photographs are limited in their spectral information and contain radiometric distortions that usually results in a lower digitized image data quality compared with digital imaging systems (Herold et al., 2002).

Remote sensing data with high resolution is now available from the IKONOS multispectral space borne sensor and are considered to be a significant advancement in remote sensing technology (Herold et al., 2002). IKONOS has a spatial resolution of 4 meters for the multispectral bands and 1 meter for the panchromatic band. This high resolution increases accuracy in LULC classification. However, IKONOS data is very expensive to obtain and cannot to be used to for large scale LULC classifications.

2.4.2 Image preprocessing

Precise geometric and radiometric correction is a prerequisite for remote sensing applications. Geometric rectification is the process of assigning map coordinates to images (Lillsesand et al., 2008). The images are geo-referenced using well-scattered ground control points (Mohan et al., 2011). Geometric rectification is important when producing spatially corrected maps of land use changes through time (Geyman and Baz, 2007).

Radiometric correction is necessary for correcting aberrations in data values due to distortions such as atmospheric effects and instrumentation errors. Wu et al. (2006) employed a radiometric correction method using image regression to calibrate the brightness value of each pixel of the subject scene to a reference image. This method minimized the differences in sun angle, earth-sun distance, atmospheric effects, detector calibration differences, and soil moisture (Wu et al., 2006; Mundia and Aniya, 2006). After removal of all distortions in images, the changes in brightness values can be attributed solely to the changes in surface conditions (Mundia and Aniya, 2006).

2.4.3 LULC Image Classification

Image Classification methods are usually divided into three major groups based on the fundamental unit of analysis: pixel-based classification, sub-pixel based classification and object-based classification methods (Li et al., 2014). The pixel-based classification assumes that each pixel belongs to a single LULC type. Pixel-based classification methods are divided into supervised, unsupervised and hybrid methods. Unsupervised classification does not require training data as the basis for classification. It takes into account algorithms that examine the unknown pixels in an image and aggregate them into a number of clusters based on natural groupings or clusters present in image values. Mundia and Aniya (2006) used unsupervised classification after obtaining their images from Landsat multi-spectral sub-system (MSS), Thematic Mapper ™, Enhanced TM (ETM). Unsupervised classification allowed identification of spectral clusters with a high degree of objectivity. The ISODATA (Iterative Self-Organizing Data Analysis) algorithms in ERDAS Image were used to identify spectral clusters. This method uses a minimum spectral distance to assign a pixel to a cluster. They yielded a producer accuracy of 85%.

In a supervised classification, different classes of LULC are known and defined in advance and their properties are learned from collected training samples. Then, all the training data are used to develop the classification model. Keuchel et al. (2003) used the supervised classification algorithm for Tenerife Island. They compared maximum likelihood based supervised classifications given different parameters. Support vector machines do not attempt to model the distribution of data but separate the various classes by searching for acceptable boundaries between them (Keuchel et al., 2003). Supervised classification methods are more

effective in identifying complex land cover classes if a priori knowledge of the study area is available, and good training data can be extracted from the image (Kuremmerle et al., 2006).

Hybrid classification combines unsupervised and supervised classification techniques and often leads to better performance. Kuremmerle et al. (2006) first performed an unsupervised clustering for each training dataset to detect datasets that will be best handled separately. The unsupervised classification data was then used as the input data for supervised classification method. They derived a land cover map using Landsat TM and ETM images and achieved an accuracy of 90%. However, the drawback to this is the complex variability in spectral response patterns of the different LULC (Lillsesand et al., 2008).

Sub-pixel based techniques view each pixel as being mixed, and the areal proportion of each class is estimated. These include fuzzy classification, neural networks (Li et al., 2014). These methods require high spatial resolution images to calculate fractions of LULC classes within pixels. Object-based classification methods first conduct segmentation of images for a study area, resulting in homogeneous polygons that are considered as objects, and then do classifications of the objects. This method has been realized in E-cognition and ArcGIS Feature Analyst (Li et al., 2014).

2.4.4 LULC Change detection

Change detection is the process of identifying differences in the state of an object or phenomenon by observing it at different times (Singh, 1989). Change detection can be applied to many studies such as LULC change analysis, damage assessment, crop stress detection (Singh, 1989). Various techniques of LULC change detection have been developed during the past several decades and are divided into post-classification based and pre-classification based

methods (Wang et al., 2004).Selection of LULC change detection techniques depends on the data availability, geographic area of study, time and computing constraints of applications (Seto et al., 2002).

Post classification based methods use remotely sensed datasets that are acquired at different times separately, generate an LULC map for each time, then compare the LULC maps and finally create an LULC change map for each pair time. These methods are efficient in detecting nature, proportion and location of changes that occur (Mundia and Aniya, 2006; Wondrade et al., 2014). Mundia and Aniya (2006) used this kind of method to analyze LULC changes and degradation of Nairobi City, Kenya. Their data was obtained in different seasons from different sensors with different spatial resolutions. Post classification based methods are by far most commonly used for LULC change detection (Wondrade et al., 2014). They do not require minimizing the problems of atmospheric and sensor differences between the two dates and accurate registration of multi-date images (Singh, 1989), but require very high accuracy of classification for each LULC map. Li et al. (2004) monitored land development in the Pearl River Delta using a post-classification based method and Principal Component Analysis (PCA). This technique combined with interactive classification was used to overcome the problem of overestimation of LULC change and also to reduce the possibilities of creating unlikely classes (Li et al., 2004).

An example of pre-classification based methods is image differencing in which the spatially registered images from the two dates is subtracted band by band on the basis of pixels. The threshold boundaries between the change and stable pixels are found for the difference image to produce the change map (Song et al., 2001). Madanian et al. (2012) found this method was the most accurate one when monitoring LULC of Falavarajan, Isfahan, Iran, as compared to

image rationing and image regression. The differencing images are often obtained using Normalized difference vegetation index (NDVI). It is a commonly used index for the analysis of vegetation in remote sensing (Gao, 1996; Singh, 1989). It is calculated using the formula NDVI = (NIR - RED) / (NIR+RED). NIR is the reflectance of the object in the near infrared band and RED is the reflectance of the object in the red band. Image ratios of the same bands at different times can also be calculated to detect LULC changes (Lu et al., 2003; Singh, 1989). Also, image regression establishes the relationship between the two images from different dates and determines the pixel values of the second image by using a regression function and then subtracts the regressed image from the first date image (Lu and Weng, 2007). This method calibrates the images from different times to the same level and thus provides the potential to improve LULC change detection.

CHAPTER 3

MATERIALS AND METHODOLOGY

3.1 Study area

The study was undertaken in Kampala, the capital and largest city of Uganda. Kampala is located at 0.3136° N and 32.5811°E and has an elevation of 1190 meters. Kampala consists of 176 square kilometers of land and 13 square kilometers of water (Figure 1a). Five administrative units make up Kampala namely Kawempe, Nakawa, Central, Rubaga, and Makindye divisions (Figure 1b). Kampala has a tropical climate with two rainy and two dry seasons. The rainy seasons are from March to May and September to November and the dry seasons are from December to February and June to August (Figure 2). The average temperature of Uganda is 28^0C in the dry season and 25^0C in the rainy season (Figure 3).

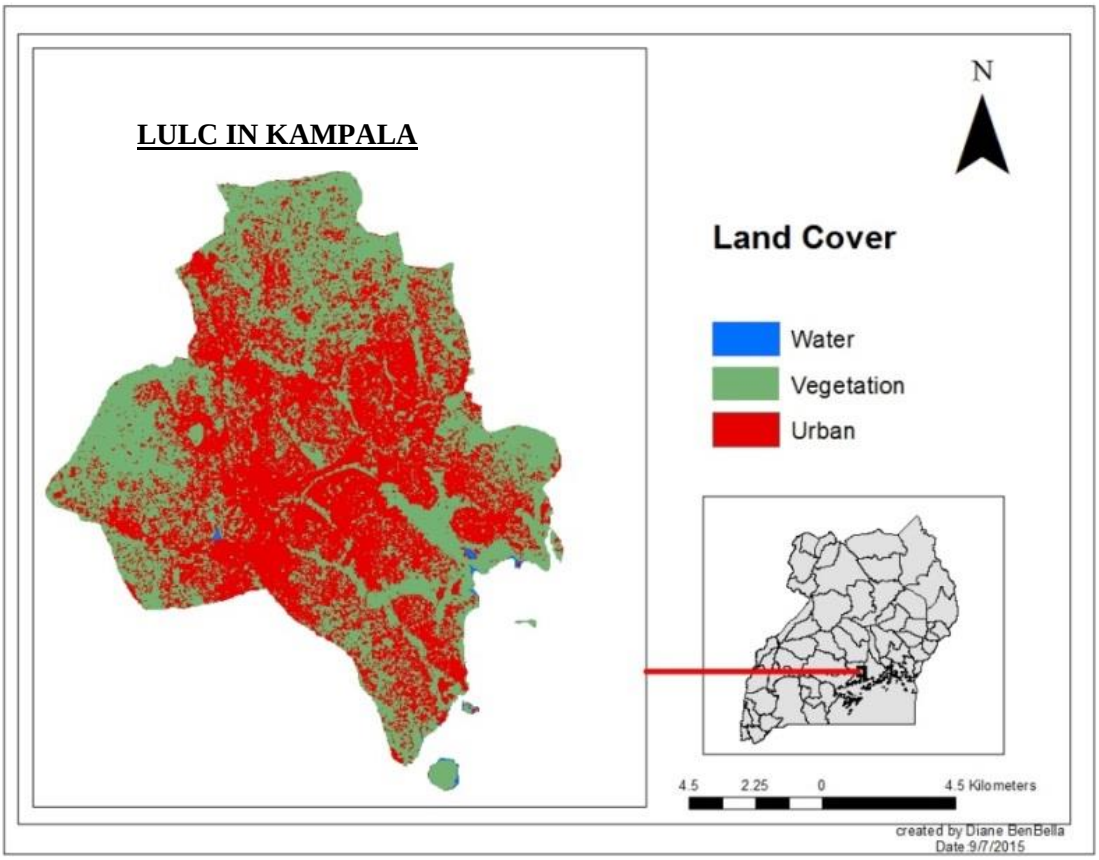
LULC IN KAMPALA
N
Land Cover
Water
Vegetation
Urban
4.5
2.25
0
4.5 Kilometers
created by Diane BenBella
Date 9/7/2015

(a)

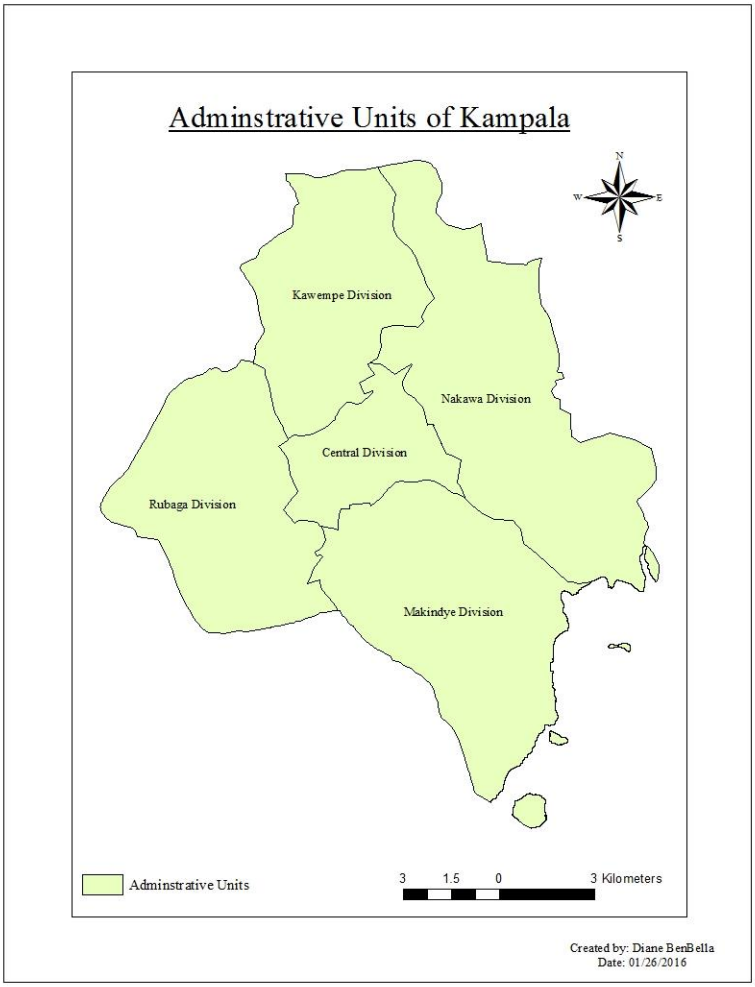

(b)

Figure 1: a) Study area and Land Use Land Cover (LULC) Categories, and b) Administrative units of Kampala.

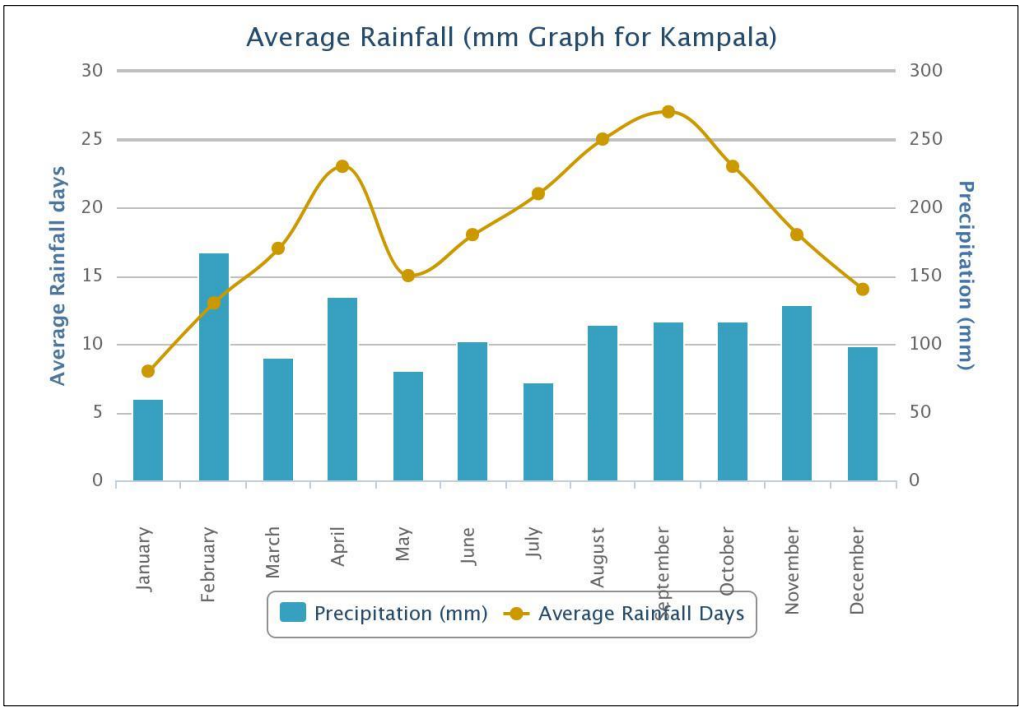

Figure 2: The average rainfall of Kampala district throughout the year (https://weather-and-climate.com/).

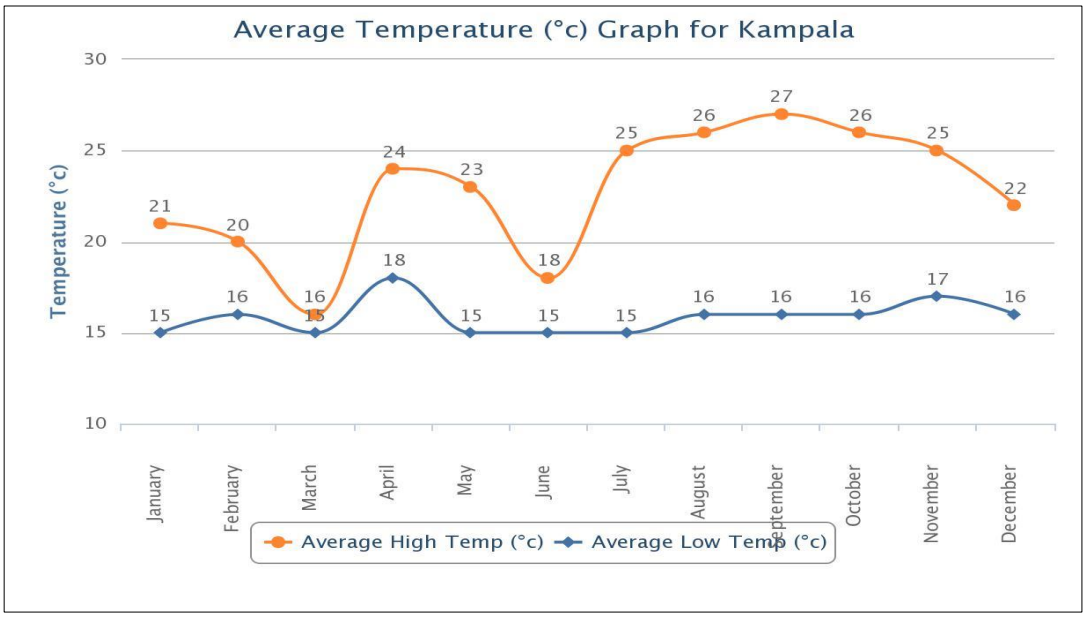

Figure 3: The average temperature of Kampala district throughout the year (https://weather-and-climate.com/).

3.2 Datasets

3.2.1 Remotely Sensed Data

Landsat 5 Thematic Mapper ™ images for the years 1995 and 2010 and a Landsat 8 Operational Land Imager (OLI) and Thermal Infrared Sensor (TIRS) image for the year 2015 were downloaded from Earth Explorer (http://earthexplorer.usgs.gov/) at no charge. The acquisition dates, the sensor and the paths and rows for the Landsat images are provided in Table 1. Band information for the three Landsat images is presented in Tables 2 and 3.

Table 1: *Information of Landsat images used.*

Sensor	Path/ Row	Acquisition Date
Landsat 5 TM	171/60	19-Jan-1995
Landsat 5 TM	171/60	28-Jan-2010
Landsat 8	171/60	27-Feb 2015

Table 2: *Band information for Landsat 5 Thematic Mapper™.*

Landsat 5	Wavelength (micrometers)	Resolution (meters)
Band 1	0.45-0.52	30
Band 2	0.52-0.60	30
Band 3	0.63-0.69	30
Band 4	0.76-0.90	30
Band 5	1.55-1.75	30
Band 6	10.40-12.50	120
Band 7	2.08-2.35	30

Table 3: *Band information for Landsat 8 Operational Land Imager (OLI) and Thermal Infrared Sensor (TIRS).*

Bands	Wavelength(micrometers)	Resolution (meters)
Band 1 - Coastal aerosol	0.43-0.45	30
Band 2 - Blue	0.45-0.51	30
Band 3 - Green	0.53-0.59	30
Band 4 – Red	0.64-0.67	30
Band 5 - Near Infrared (NIR)	0.85-0.88	30
Band 6 - SWIR 1	1.57 - 1.65	30
Band 7 - SWIR 2	2.11 - 2.29	30
Band 8 - Panchromatic	0.50 - 0.68	30
Band 9 - Cirrus	1.36 - 1.38	30
Band 10 - Thermal Infrared (TIRS) 1	10.60 - 11.19	100
Band 11 - Thermal Infrared (TIRS) 2	11.50 - 12.51	100

The choice of these dates depended on the following factors: availability of the data sets, the presence of clouds in the study scene and the climatic season. The dry season was preferred because there was minimum cloud coverage during this time, so I was able to obtain cloud free Landsat images**.**

A total of five aerial photographs with a spatial resolution of 0.5 meters were obtained from the Department of Land Surveys, Uganda. Each of the photographs consisted of three bands and was acquired on February 2, 2015. These aerial photographs were mosaicked into one photograph to show Kampala in its entirety. The mosaicked image was useful in the geometric correction process and accuracy assessment after image classification had been carried out.

3.2.2 Population and socio-Economic Data

The current population of Kampala is 1.9 million with a growth annual rate of 5.7% (World Bank, 2013). The average income of a household in Kampala is approximately 5,000 dollars to 10, 000 dollars a year (Uganda National Household Surveys Report, 2010). This was an improvement from 2005 when the average household income was 1527 (Uganda National Household Surveys Report, 2010).

The urban aspect of Kampala is divided into two forms: local *kibuga* and Kampala Township. The local *kibuga* includes the unplanned structures characterized by poor sanitation and drainage such as Bwaise. The Kampala municipality includes the well-planned areas such as Kololo, Muyenga, Gaba, and Bunga. LULC in Kampala presently covers a wide area of built up area, wetlands, forest, shrubs, and urban agriculture.

The socio-economic data (Table 4) used in this study investigated the drivers of LULC. These factors were based on past urbanization studies and include population, economic growth measured in GDP per capita, and foreign direct investments (Yuanbin et al., 2012; Seto and Kaufmann, 2003). Uganda Bureau of Statistics, and World Bank provided this data.

Table 4: *Social Economic data for Uganda from 1995 to 2013*.

Year	GDP per capita(US $)	Uganda Population in millions	Kampala population	Foreign direct investments (US $)
1995	227.51	20.74	725697.3	121200000
1996	282.36	21.41	754364.4	121000000
1997	283.88	22.08	783713.7	175000000
1998	289.36	22.78	814150.5	210000000
1999	255.17	23.51	846069.3	140200000
2000	255.12	24.28	879894.9	160700000
2001	232.8	25.09	915738.3	151496151
2002	238.16	25.94	953655	184648059
2003	236.11	26.84	1005072.3	202192594
2004	285.96	27.77	1062503.7	295416480
2005	313.8	28.72	1122941.4	379808341
2006	334.64	29.71	1186643.4	644262500
2007	400.04	30.73	1253733	792305781
2008	448.07	31.78	1324413.3	728860901
2009	517.1	32.86	1398935.7	841571803
2010	553.3	33.99	1477628.1	543872727
2011	530.9	35.15	1560573.9	894293858
2012	652.7	36.35	1648103.1	1205388488
2013	657.4	37.58	1740315.3	1194398346

3.3 Methodology

The methodology (Figure 4) consisted of the following steps: collection and processing of the Landsat TM and OLI images; image classification using SMA and ANN and then determination of the accuracy of each of the classification methods; detection and quantification of the LULC changes that have occurred between 1995 and 2015; determination of the factors that affect urbanization; and estimation of the land cover transition in the next fifteen years using Markov simulation.

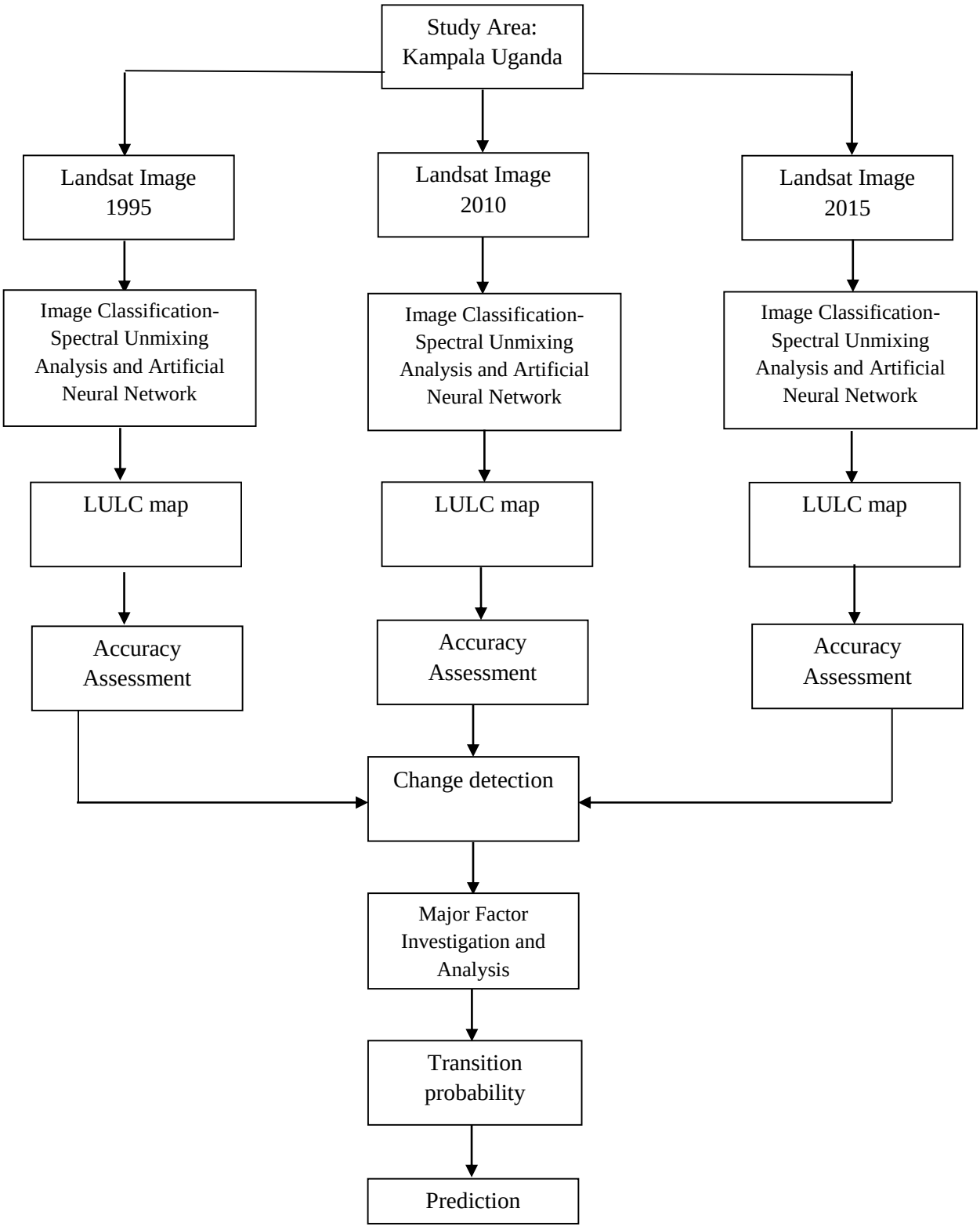

Figure 4: Methodology framework.

3.3.1 Image preprocessing

Before any change detection can be conducted using remote sensing technology, the data have to be preprocessed. Image preprocessing improves data analysis by ensuring that all datasets have the same spectral and spatial resolution as well as having the same coordinate system. The three Landsat images were geometrically corrected to WGS_1984_UTM_Zone_36N. The 1995 Landsat image was geometrically rectified using the aerial photograph. Ten Ground Control Points (GCPs) and six independent checkpoints were located on both the Landsat image and the aerial photograph. A second order polynomial was applied, resulting in a Root Mean Square Error (RMSE) of less than one pixel. The image was resampled to a pixel size of 30 X 30 using the bilinear interpolation method to maintain the properties of the original image. The other two Landsat images were co-registered to the 1995 Landsat image, using a second order polynomial and bilinear interpolation resampling method, with the RMSEs of 1.2 and 0.9 pixels obtained.

3.3.2 Image Classification

Based on the ancillary data, local knowledge and the Anderson et al. (1972) classification scheme, four LULC cover classes were identified: urban areas, subsistence agriculture, vegetation, and water. The urban LULC encompassed residential houses, industries, and transportation and communication systems. Vegetation consisted of forests, wetlands and grass including golf courses, and lawns. Water consisted of permanent open water, lakes, and reservoirs. Subsistence agriculture consisted of urban farming for commercial and private use. Images were classified using two methods: SMA, a linear based classification method, and ANN, a non- linear based classification method. ANN and SMA were chosen because of their ability to classify mixed pixels that dominated the city landscape. Hard classification technologies would

not yield accurate results because of their tendency to assign a single pixel with a given class that is acceptable for pure pixels but very misleading for the pixels that contain more than one category. These two methods were then compared to each other to determine which one would produce superior classification.

3.3.2.1 Artificial Neural Network (ANN)

ANN is a branch of artificial intelligence that are inspired by the Central Nervous System of animals (Jain et al., 1996). ANNs are viewed as weighted directed graphs in which nodes and weights connect the input layer to the output layer (Jain et al., 1996). ANNs can be categorized into feedforward networks and feedback networks (Jain et al., 1996). Feed forward networks are typified by having no loops, being static and memory-less that is the response to an output is independent of the previous network state. Examples include the single layer perceptron, the multi-layer perceptron, and the Radial Basis Function Nets. Feedback networks possess these loops and are dynamic as a result of feedback connections. These feedback connections also cause the input to be modified as neuron outputs are computed (Jain et al., 1996). Examples include Hopfield networks and Kohonen's Self-Organizing Mapper (SOM). The Hopfield neural network is a single layer recurrent neural network, and it is typically used for pattern recognition. The algorithm utilized in this neural network trains it to recognize patterns. The Hopfield indicates recognition of patterns by echoing it back. SOM is an unsupervised learning model that will classify units with similar patterns to the same class (Dian Pratwi, 2011). Unlike other neural networks that employ error-correction training, SOM applies competitive learning and contains only two layers. It possesses no hidden layer. (Jain et al., 1996).

Multi-Layer Perceptron (MLP) is the most widely used neural network for land cover classification mainly because of its simplicity (Bischof et al., 1992; Civco, 1993; Serpico et al.,

1996 and Chen et al., 1997). It is made up of three layers: an input layer, a hidden layer, and an output layer. The MLP uses different algorithms to calculate weights for each input value at each node as data is fed into the network (Pijanowski et al., 2005).The output of each node is a function of its input, and this feature is referred to as an activation function and can take on many different forms (Pijanowski et al., 2005). The most popular algorithm used under the MLP for calculation of weights is the Backpropagation (BP) algorithm (Pijanowski et al., 2005).

The BP algorithm randomly selects the initial weights and then compares the calculated output for a given observation with the expected output for that observation. The difference between the expected and calculated output values across all observations is summarized using the mean squared error. After presentation of all observations to the network, the weights are then modified according to a generalized delta rule:

$$\Delta w = \eta(t-u)\frac{x}{x^2} \qquad (1)$$

whereby Δw is the modified weight, η is the learning rate, t-u is the difference between actual outputs and expected outputs, and x is the value of an input at a particular node (Pijanowski et al., 2002b).The process of presenting data to the neural net with input and output data over repeated cycles is known as training. The ANN classification for this study was conducted using Terrset IDRISI software.

3.3.2.2 Spectral Mixture Analysis (SMA)

SMA models image pixel spectra as a linear combination of endmembers (pure pixels) and is used to obtain the fractional contribution of endmembers to an image pixel spectra in a broad range of applications most especially LULC in an urban context (Denninson and Roberts, 2003). The underlying assumption of the SMA model is that there is no significant amount of multiple scattering between the different LULC types; each photon that is recorded by the sensor has interacted with only one cover type. As a result, the total energy received by the sensor can be considered to be the sum of the energies reflected by all LULC classes (Settle J.J and Drake N.A, 1993). Likewise, the reflectance of a pixel $\acute{\rho}_\lambda$ is determined by the sum of the reflectance values of all the endmembers within a mixed pixel multiplied by its fractions:

$$\acute{\rho}_\lambda = \sum_{i=1}^{N} f_i \; X \; \rho_{i\lambda} + \varepsilon_\lambda \qquad (2)$$

where $\rho_{i\lambda}$ is the reflectance of endmember *i* for a particular band (λ), f_i is the fraction of the endmember, N is the number of endmembers, and ε_λ is the residual error (Denninson and Roberts, 2003).The modeled fractions of the endmembers are limited to one unit:

$$\sum_{i=1}^{N} f_i = 1 \qquad (3)$$

Model fitness is assessed using the model residual ε_λ or the root mean squared error (RMSE)

$$\text{RMSE}\sqrt{\frac{\sum_{\lambda=1}^{M}(\varepsilon_\lambda)^2}{M}} \qquad (4)$$

where M is the number of bands (Denninson and Roberts, 2003).

SMA was implemented using ENVI software. The three Landsat images were selected as input data. The unmixing process involved the following steps: (1) determining the inherent

dimensionality of the data using the Minimum Noise Fraction (MNF) transform; (2) deriving the Pixel Purity Index (PPI) in order to identify endmembers; (3) Selecting pure pixels with the n-D Visualizer; (4) Developing a model with the pure pixels and applying it to Kampala.

3.3.3 Change detection

The LULC changes from 1995 to 2015 were assessed using post-classification analysis. This involved comparing the independently classified maps with each other (Singh, 1999). Post classification analysis generated a complete matrix of changes that were helpful in determining the changes that occurred and identifying the changes of interest. This part of the methodology was carried out using Land Change Modeler software tool in TerrSet IDRISI. It compared the classified LULC map of 1995 with the classified map of 2010, the classified map of 2010 with the map of 2015 and finally the classified map of 1995 with the classified map of 2015.

3.3.4 Markov Chain Simulation

Markov chain analysis was implemented to estimate the land cover transition. The Markov chain analysis is defined as a stochastic process having the property that the state at time t2 is derived from the knowledge of its state at an earlier time t1 and is not dependent on the history of the system before t1 (Mubea et al., 2011). Markov chains have been used to model changes in LULC at a variety of spatial scales (Weng, 2002). LULC change is a deterministic process, and designing models for such a process is difficult. To apply Markov simulation to LULC, we assume that the process is stochastic, and the different categories are the states of the chain (Mubea et al., 2011). It is also important to regard the change process as one that is discrete in time. The equation of Markov chain analysis is:

$V_{t2} = P \times V_{tl}$ (7)

where V_{t1} is the input LULC proportion column vector, V_{t2} is the output LULC proportion column vector, and P is an m x m probability transition matrix for the time interval $\Delta t = t2 - t1$ and constructed using the probability:

$$p_{ij} = \frac{n_{ij}}{n_n}, \qquad i, j = 1,2,...k$$

where n_i = the total number of pixels that changed from one class in the first image to another class in the simulated image and n_{ij} = the number of pixels of class *i* from the first map that were changed to class *j* in the second map and *k* is the total number of classes. (Mubea et al., 2011; Chen et al., 2013). The transition matrix shows the likelihood of each category to change or remain the same in the next period (Weng, 2002).

The Markov module considers LULC changes between two classified maps of different years as input to generate a probability matrix that shows the probability of each category changing or remaining the same in another time period (Eastman, 2012). The probability matrix is then used to obtain a transition area matrix that shows the quantity of cells that are expected to change. In this study, the classified maps of 1995 and 2010 were used to predict the LULC of 2015 using a probability matrix. The simulated map of 2015 was then compared to the actual classified map 2015 to determine the accuracy of the model. Once the simulated map was validated, a prediction map of the year 2025 was generated using the same transition matrix. 2025 was an ideal year for the prediction because of the same time period as the one used to produce the transition matrix.

To carry out Markov simulation for this study, explanatory variables, that is, factors that drive LULC changes, were selected. Based on previous studies, two most common variables, namely distance to roads and distance to previous disturbance, were selected. Distance to disturbance was defined as the distance to previous urbanized areas. Land Change Modeler in IDRISI Terrset divided them into static and dynamic variables. Distance from roads is a static variable since the distance from the main roads is less likely to change over time. Distance to previous disturbance is dynamic because it changes from one year to the next. A distance to roads map was created by conversion of the roads vector layer of Kampala to a raster format using the RASTERVECTOR module and then running the DISTANCE module on the result. For the distance to previous disturbance map, the first step involved extraction of the disturbed areas from the previous land cover image. The next step was filtering the resulting image with a 3×3 mode filter to remove extra pixels and then running the DISTANCE module on the result. These maps were tested using the Cramer's *v* to determine the ability of the variables to effect change (Table 5). A Cramer's *v* is a quantitative measure of association between two variables. A high Cramer's *v* indicates that the potential explanatory value of the variable is strong but does not necessarily assure good performance of the model (Clark Labs, 2009). Cramer's v values of 0.15 and above are considered useful to run the analysis.

Table 5*: Explanatory variables and their Cramer's V*.

Variable	Cramer's V
Distance from roads	0.2498
Distance from previous disturbance	0.3582

After selection of the explanatory variables, the Multi-Layer Perceptron Neural Network was used as the transition to build the relationship between the explanatory variables and the transition and persistence classes that were used as weights in the model. The neural network divided the pixels to be evaluated into two parts. One part was used to train the model and the other to validate the model. As it continued to analyze the pixels, it determined the error and adjusted the weights accordingly with the aim of improving accuracy and precision. The accuracy rate measures the accuracy and the Root Mean Square Error measures the precision of the model.

3.3.5 Factors affecting City sprawling

GDP per capita and FDI also had considerable influence on city sprawling and were analyzed using Pearson product-moment correlation. The correlation coefficient is a measure of the strength of a linear association between two variables and is denoted by *r* with a range of values from +1 to -1. A value of 0 indicates that there is no association between the two variables. A value greater than 0 indicates a positive association and a value less than 0 indicates a negative association. For this study, the correlation between GDP per capita and the percentage increase in urban areas as well as FDI and the percentage increase in urban areas for the period 1995 to 2013 was calculated.

3.3.6 Accuracy Assessment

3.3.6.1 Accuracy assessment of classification

Accuracy assessment determines the quality of a classification map generated from remotely sensed data. The accuracy of a classification is usually assessed by comparing the classification map with a reference map/ image that is believed to show a true depiction of LULC

or to have a higher accuracy for the study area. The error matrix is perhaps the most widely used accuracy assessment method in remote sensing and it generates the overall accuracy, the accuracies of each category, the omission and commission error and the Kappa Index. Accuracy Assessment for this study was carried out using the ERDAS Imagine software. Past aerial photographs and Google images were utilized as the reference images for my accuracy assessment.

3.3.6.2 Accuracy Assessment of the Markov simulation.

Comparison of the simulated map 2015 with the classified map 2015 was used to determine the accuracy of the Markov simulation. There are two ways to carry out the comparison. One method was to compare the cell by cell agreement regarding location and quantity of the simulated map with the classified map using the VALIDATE module in TerrSet. The VALIDATE module generates various Kappa Indices of Agreement that determine how well the comparison map agrees with the reference map. The standard Kappa index ($K_{standard}$) compares the correct observed proportion to the correct expected proportion (Pontius, 2000).It determines whether the model is valid or not. The kappa index for a valid model is usually greater than 70 %. The module also produces other kappa indices of agreement such as the Kappa for no information (K_{no}), the Kappa for grid cell location ($K_{location}$) and the Kappa for stratum- level location (Pontius, 2000). The Kappa for no information indicates the proportion that is correctly classified relative to the expected proportion classified correctly by simulation with no ability to specify accurately quantity or location (Araya and Cabral, 2010). Kappa for location is defined as the success due to a simulation's ability to specify location divided by the maximum possible success due to a simulation's ability to specify location perfectly (Araya and Cabral, 2010). Another validation of the Markov simulation is the analysis of a validation map

generated from the validation option within the Land Use Change Model tab in TerrSet. This tab runs a three cross tabulation between the later land cover map in the input, the prediction map that was created and the map of reality. The validation map is then generated displaying the following information: The number of misses which depict places where the model failed to predict urban expansion, the false alarms that show regions where the model tended to overpredict urbanization expansion and the hits that depict areas where the model accurately predicted urban expansion.

CHAPTER 4

RESULTS

The results are divided into four sections: the results of two classification methods for the three years; the observed changes of LULC between the time periods; the results of Markov simulation; and the main drivers of urbanization in Kampala.

4.1 Image classification and accuracy assessment

4.1.1 Artificial Neural Network (ANN)

Figure 5 shows 1995, 2010, and 2015 classification maps for Kampala using ANN. There is an observable change in LULC between 1995 and 2015. From the three maps, we can see the direction and the magnitude of urban expansion. The urbanized areas have expanded tremendously over the last 20 years, and the expansion is more towards the Northern and Western parts of the city. Vegetated areas have decreased over the three temporal periods but not as significantly as agriculture lands that have been replaced with urban areas. Water showed no significant form of change.

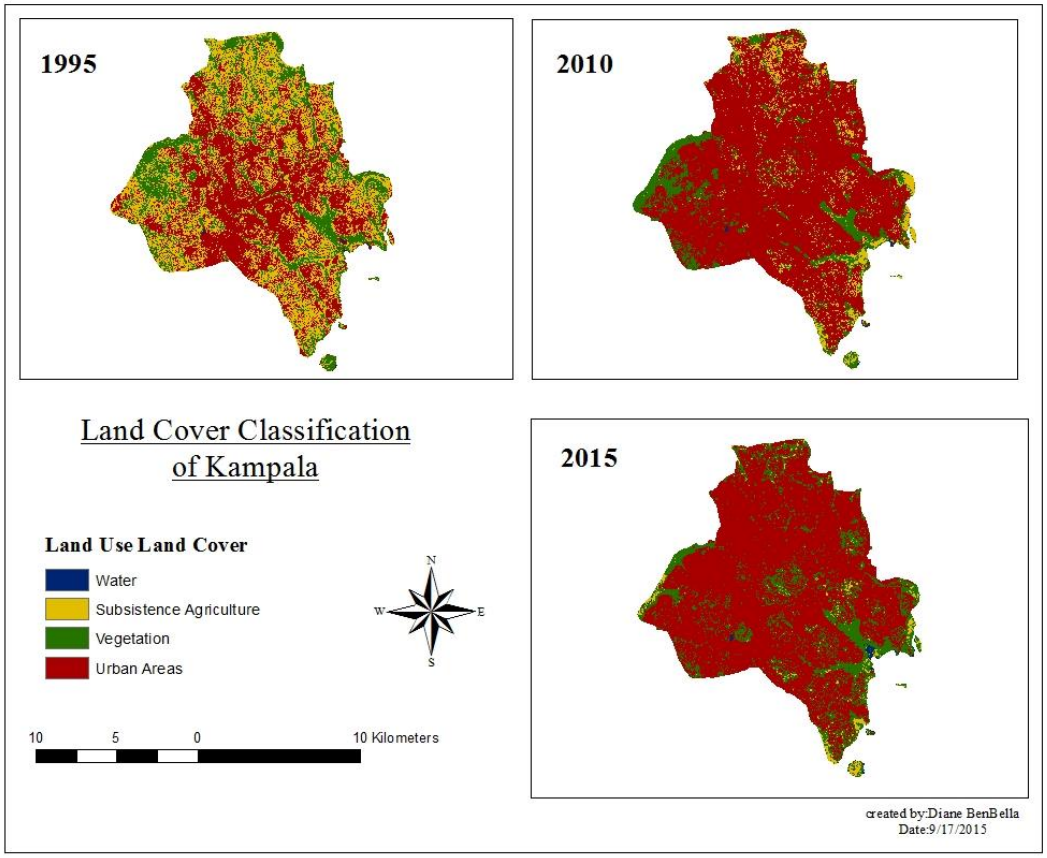

Figure 5: ANN classification of Kampala for the years 1995, 2010 and 2015.

4.1.1.1 ANN Accuracy Assessment

Error matrices of the three classified maps using ANN were created by comparison with the reference images. The matrices were then used to assess classification accuracy. We derived the producer's accuracy, user's accuracy, overall accuracy, kappa coefficient, and the overall kappa value from the error matrices. A total of 160 pixels obtained from the stratified random sampling design were used to determine the accuracy.

The overall accuracy of the 1995 ANN classification was 85.63% (Table 6). This was the highest classification accuracy of the three years and showed an excellent agreement of classification by the Landsat data with the reference image. The producer's accuracy was 100%,

80.77 %, 80.77%, and 93% for water, subsistence agriculture, vegetation, and urban, respectively, which represents the omission errors. The corresponding user's accuracy was 100%, 84%, 84%, and 86%, respectively, implying the commission errors. Subsistence agriculture and vegetation both had the greatest omission errors of 19.23 % for the pixels classified into other categories. Subsistence agriculture had its pixels classified as either vegetation or urban areas. Vegetation had its pixels classified as either subsistence agriculture or urban areas. Urban areas had 7% of its pixels classified as either subsistence agriculture or vegetation. The presence of omission errors is due to the Kampala landscape being dominated by mixed pixels. Water had no omission error. Vegetation, subsistence agriculture, and urban areas had commission errors indicating they had pixels that were classified into that category but, in fact, belonged to another category. Water was accurately classified in this year since it had no commission and omission errors. The kappa coefficient was 0.7956, which indicates the agreement between the classified and reference image was 79.56% better than that by chance.

Table 6*: Error matrix of 1995 ANN classification.*

	1995	Reference Image						
		Water	Subsistence Agriculture	Vegetation	Urban Areas	Xi+	UserA	C.K
Classified Map	Water	10	0	0	0	10	100%	1
	Subsistence Agriculture	0	42	6	2	50	84%	0.763
	Vegetation	0	7	42	1	50	84%	0.763
	Urban Areas	0	3	4	43	50	86%	0.8035
	X+j	10	52	52	46	160		
	Prod A	100%	80.77%	80.77%	93%			
	Overall classification Accuracy = 85.63% Overall Kappa ststistics= 0.7956							

The overall accuracy of the 2010 ANN classification was 83.75% (Table 7).The producer's accuracy was 100%, 87.23%, 84%, and 78% for water, subsistence agriculture, vegetation and urban areas, respectively, representing the omission errors. Their corresponding

user's accuracy was 90%, 82%, 82%, and 86% representing the commission errors. Urban areas had the largest omission error with 22% of its pixels being classified into other LULC categories. Vegetation had the second largest omission error with 16 % of its pixels being classified into other LULC categories. Subsistence agriculture had an omission error of 12.77%. Water had no omission error. All the LULC categories had commission errors indicating they had pixels that were classified into that category but, in fact, belonged to another category. Subsistence agriculture and vegetation had the greatest commission error with 18 % of their pixels belonging to other categories while water and urban areas had 10 % and 16 % of their pixels wrongly classified. The Kappa coefficient was 0.7684 which indicates that the agreement between the classified and reference image was 76.84 % better than that by chance.

Table 7: *Error matrix of 2010 ANN classification*.

	2010	Reference Image						
		Water	Subsistence Agriculture	0	Urban Areas	Xi+	UserA	C.K
Classified Map	Water	9	0	0	1	10	90%	0.894
	Subsistence Agriculture	0	41	6	1	48	82%	0.7451
	Vegetation	0	7	41	5	53	82%	0.7405
	Urban Areas	0	3	3	43	49	86%	0.7867
	X+j	9	51	50	50	160		
	Prod A	100%	87.23%	84.00%	78%			
	Overall classification Accuracy = 83.75% Overall Kappa ststistics= 0.7684							

The overall accuracy of the 2015 ANN classification was 82.50% (Table 8). Compared to the accuracy for the years 1995 and 2010, this accuracy was much lower. The producer's accuracy was 100%, 86.05%, 85.71%, and 74.58% for water, subsistence agriculture, vegetation, and urban areas, respectively. The corresponding user accuracy was 90%, 74%, 84%, and 88%, respectively. Urban areas had the greatest omission error with 25.42% being classified as subsistence agriculture or vegetation. The omission errors were mainly due to the prevalence of

mixed pixels that dominate the Kampala landscape. Water had no omission error. All the LULC categories had commission errors. Water, vegetation, subsistence agriculture, and urban had 10%, 26 %, 16%, and 12% of their pixels incorrectly classified. The Kappa coefficient was 0.7506 which indicates that the agreement between the classified and reference image was 76.84 % better than that by chance.

Table 8: *Error matrix of 2015 ANN classification*.

	2015	Reference Image						
		Water	Subsistence Agriculture	0	Urban Areas	Xi+	UserA	C.K
Classified Map	Water	9	0	1	0	10	90%	0.894
	Subsistence Agriculture	0	37	3	10	50	74%	0.6444
	Vegetation	0	3	42	5	50	84%	0.7694
	Urban Areas	0	3	3	44	50	88%	0.8099
	X+j	9	43	49	59	160		
	Prod A	100%	86.05%	85.71%	75%			
	Overall classification Accuracy = 82.50% Overall Kappa ststistics= 0.7506							

4.1.2 Spectral Mixture Analysis (SMA)

SMA produced three fractions images: vegetation, urban areas, and water for each of the three years (Figures 6-8). The fraction images show the proportion of each LULC category in a given pixel. In SMA, agricultural lands and vegetated areas were combined. The fraction images show the expansion of the urban area at the expense of vegetation. The fraction images were combined using the HARDEN tool in IDRISI to give overall classification maps of the years 1995, 2010, and 2015 (Figure 9). Like ANN, SMA also reveals an observable change in LULC between 1995 and 2015. From the three maps, we can clearly see the direction and magnitude of urban expansion. The LULC types have expanded tremendously over the last 20 years, and the expansion took place towards the Northern and Western parts of the city. Vegetation has shown a significant decrease and been replaced by urban. Water appears to show significant change; however, this is as a result of its misclassification.

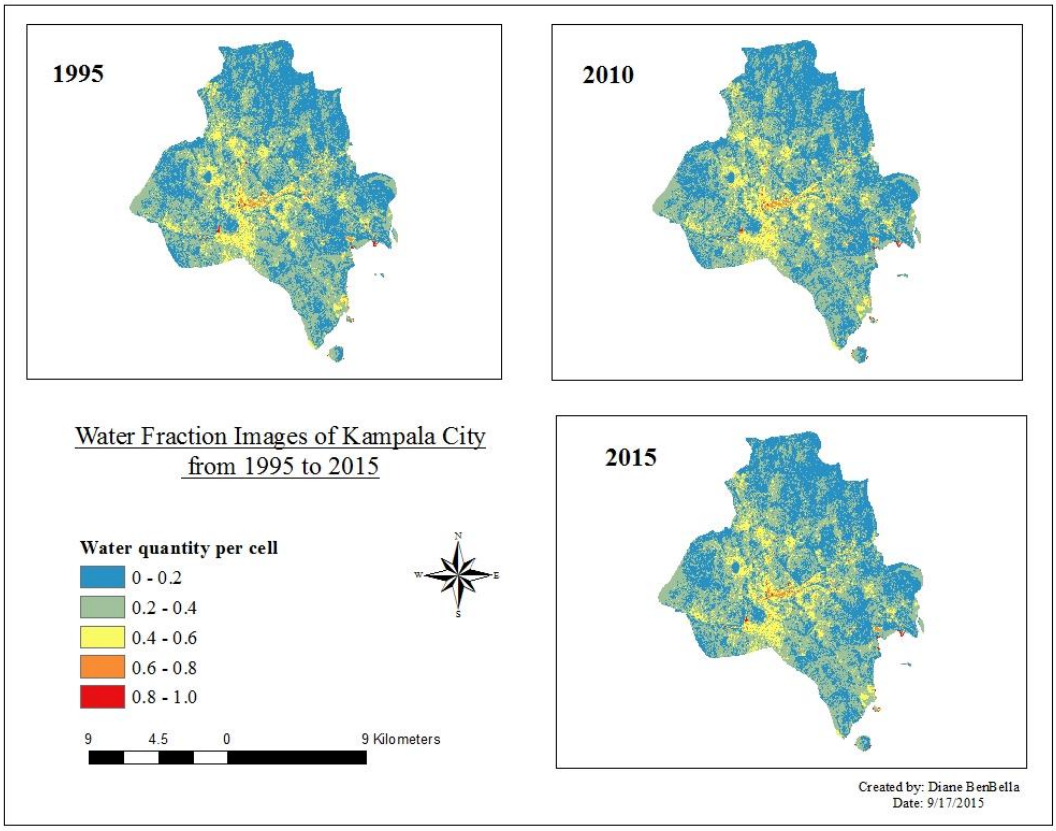

Figure 6: Water Fraction images of Kampala for the years 1995, 2010, and 2015.

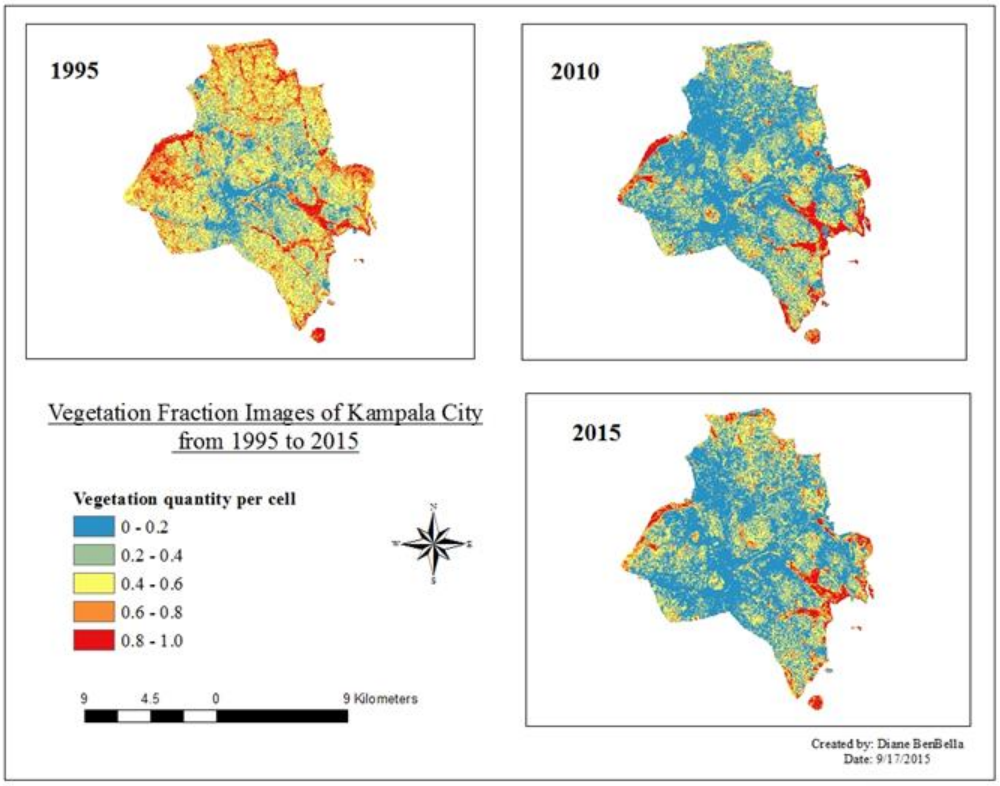

Figure 7: Vegetation Fraction images of Kampala for the years 1995, 2010, and 2015.

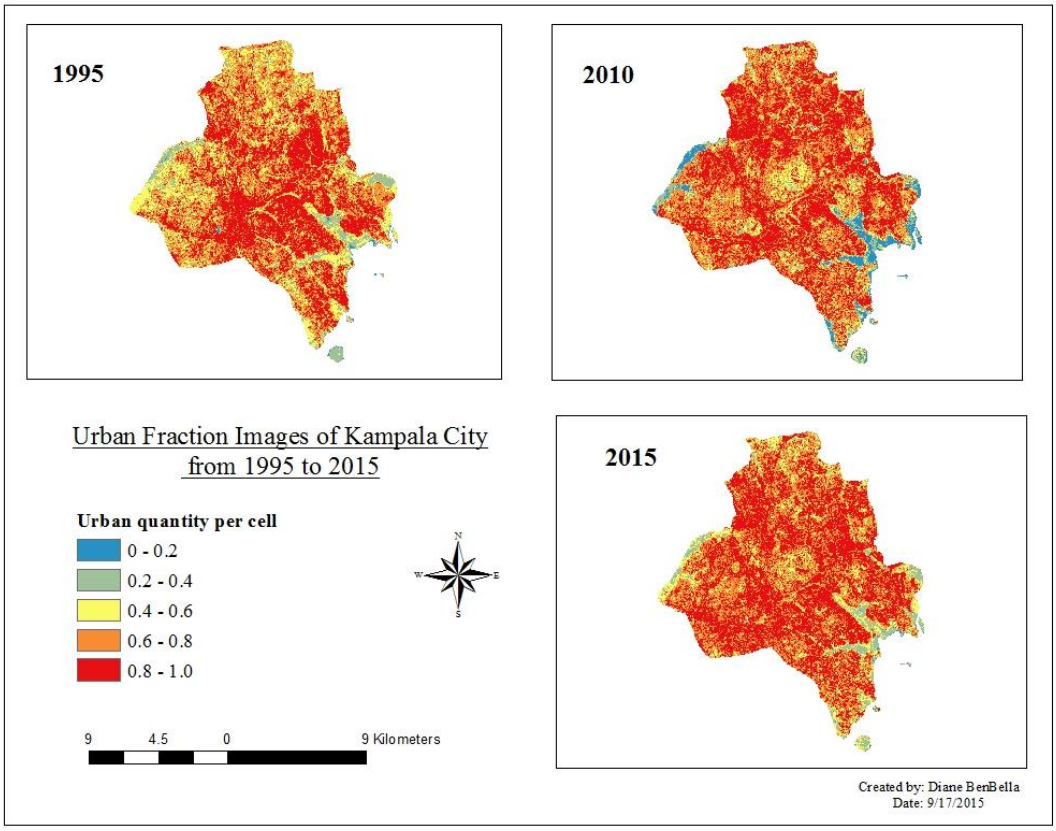

Figure 8: Urban Fraction images of Kampala for the years 1995, 2010, and 2015.

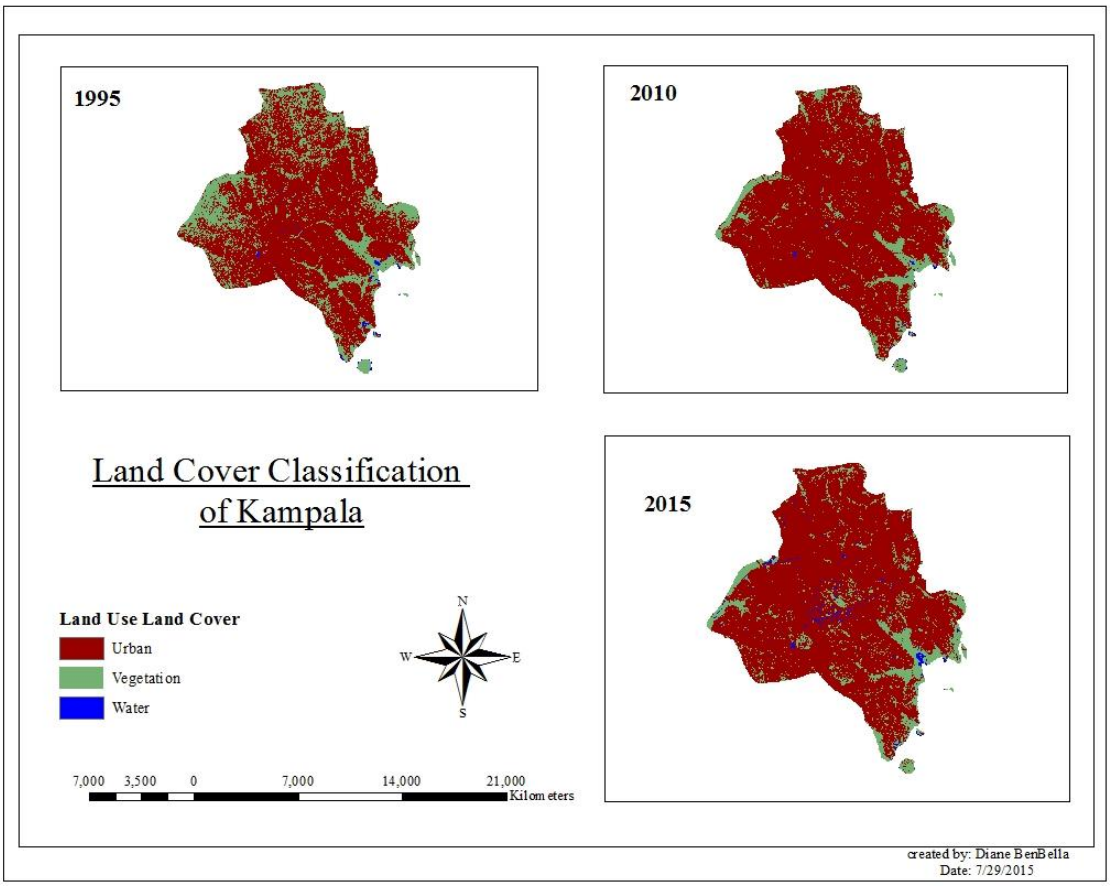

Figure 9: SMA classification of Kampala for the years 1995, 2010 and 2015.

4.1.2.1 SMA Accuracy Assessment

Error matrices of the three classified maps produced using SMA were created by comparison with the reference images. The matrices were then used to assess classification accuracy. We derived the producer's accuracy, user's accuracy, overall accuracy, kappa coefficient, and the overall kappa value from the error matrices. A total of 110 pixels obtained from the stratified random sampling design were used to determine the accuracy.

The overall accuracy of the 1995 SMA classification was 80.91% (Table 9). The producer's accuracy was 100%, 80.85%, and 77.78%, for water, vegetation, and urban, respectively, which represents the omission errors. The corresponding user's accuracy was 90%, 76%, and 84%,

respectively, implying the commission errors. Urban Areas both had the greatest omission errors with 22.22% of its pixels being classified in other classes. Vegetation had 19.15% of its pixels being classified as urban Areas. The presence of omission errors is due to the Kampala landscape being dominated by mixed pixels. Water had no omission error. All the classes had commission errors indicating they had pixels that were classified into that category but, in fact, belonged to another category. The kappa coefficient was 0.6681, which indicates the agreement between the classified and reference image was 66.81% better than that by chance.

Table 9: *Error matrix of 1995 SMA classification.*

	1995	Reference Image					
		Water	Vegetation	Urban	Xi+	UserA%	C.K
Classified Map	Water	9	1	0	10	90%	0.8911
	Vegetation	0	38	12	50	76%	0.581
	Urban Areas	0	8	42	50	84%	0.6857
	X+j	9	47	54	110		
	ProdA	100%	80.85%	77.78%			
	Overall classification accuracy=80.91%, Overall kappa statistics= 0.6681						

The overall accuracy of the 2010 SMA classification was 78.18% (Table 10).The producer's accuracy was 100%, 78.26%, and 74.07% for water, vegetation and urban areas, respectively, representing the omission errors. Their corresponding user's accuracy was 100%, 72%, and 80% representing the commission errors. Urban areas had the largest omission error with 25.93% of its pixels being classified into other LULC categories. Vegetation had the second largest omission error with 21.74% of its pixels being classified into other LULC categories. Water had no omission error. Vegetation and Urban Areas had commission errors indicating they had pixels that were classified into that category but, in fact, belonged to another category. Vegetation had the greatest commission error with 28 % of its pixels belonging to other categories while urban areas 20% of its pixels wrongly classified. Water had no commission

error.The Kappa coefficient was 0.6 which indicates that the agreement between the classified and reference image was 60 % better than that by chance.

Table 10: *Error matrix of 2010 SMA classification.*

Classified Map	2010	Reference Image					
		Water	Vegetation	Urban	Xi+	UserA%	C.K
	Water	10	0	0	10	100%	1
	Vegetation	0	36	14	50	72%	0.5188
	Urban Areas	0	10	40	50	80%	0.6071
	X+j	10	46	54	110		
	ProdA	100%	78.26%	74.07%			
	Overall classification accuracy=78.18%, Overall kappa statistics= 0.6						

The overall accuracy of the 2015 SMA classification was 76.36% (Table 11).The producer's accuracy was 100%, 76.60%, and 72.22% for water, vegetation and urban areas, respectively, representing the omission errors. Their corresponding user's accuracy was 90%, 72%, and 78% representing the commission errors. Urban areas had the largest omission error with 27.78% of its pixels being classified into other LULC categories. Vegetation had the second largest omission error with 23.4% of its pixels being classified into other LULC categories. Water had no omission error. All the LULC categories had commission errors indicating they had pixels that were classified into that category but, in fact, belonged to another category. Vegetation had the greatest commission error with 28 % of its pixels belonging to other categories while urban areas 22% of its pixels wrongly classified. The Kappa coefficient was 0.5891 which indicates that the agreement between the classified and reference image was 58.91 % better than that by chance.

Table 11: *Error matrix of 2015 SMA classification.*

Classified Map	2015	Reference Image					
		Water	Vegetation	Urban	Xi+	UserA%	C.K
	Water	9	0	1	10	90%	0.8911
	Vegetation	0	36	14	50	72%	0.5111
	Urban Areas	0	11	39	50	78%	0.5679
	X+j	9	47	54	110		
	ProdA	100%	76.60%	72.22%			
	Overall classification accuracy= 76.36%, Overall kappa statistics= 0.5891						

4.2 LULC Changes

The observed LULC changes of the three years were analyzed using IDRISI Land Change Modeler (LCM). LCM divides its results into three sections: the quantitative assessment of different LULC categories; net change of each LULC class; and the contributors to the net change experienced by each LULC category. The results are displayed using percentage change.

Percentage change = (Number of pixels that changed from one LULC category to another/ the total number of pixels of the LULC category in the later land cover image) x 100 %

The results show that subsistence agriculture, vegetation, and urban area have experienced the most change during the three temporal periods as shown in Figures 10 – 12. Water appears to have had significant change but in reality the change is very negligible. This is attributed to the fact that water occupies the smallest area in this region and as a result if one of its pixels changes to another class, the percentage change appears large. Also, the program assigned most unclassified pixels to water and this also contributed to the significant gains and losses of this category. From 1995 to 2010, urban areas experienced a net positive change of 18.77 % while subsistence agriculture and vegetation experienced a net negative change of 14.88 % and 3.91 % respectively. The main contributors to the urban increment were subsistence agriculture and vegetation. Vegetation also gained 1.21% from subsistence agriculture but lost

5.02% to urban areas. Subsistence agriculture lost its percentage area to both vegetation and urban areas with 13. 67 % lost to urban areas. From 2010 to 2015, urban experienced a net positive change of 4 % while subsistence agriculture experienced a net negative change of more than 90%, and vegetation experienced a net change of 30%. Overall between 1995 and 2015, urban experienced a net positive change of 50 % while vegetation experienced a net negative change of 10.5 % and subsistence agriculture a negative net change of more than 90%. This implies that the annual urban growth rate from 1995 to 2015 is 3.5 %.

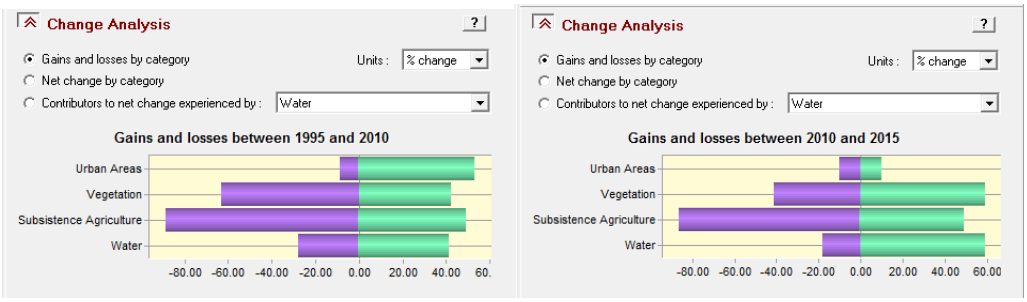

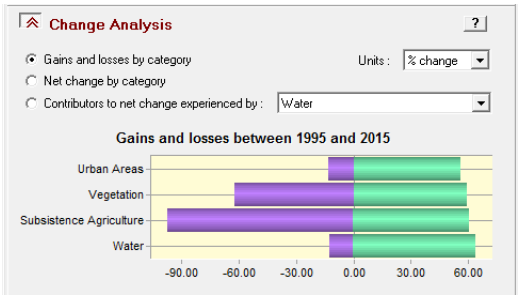

Figure 10: Gains and losses percentage change of the four LULC categories found in Kampala.

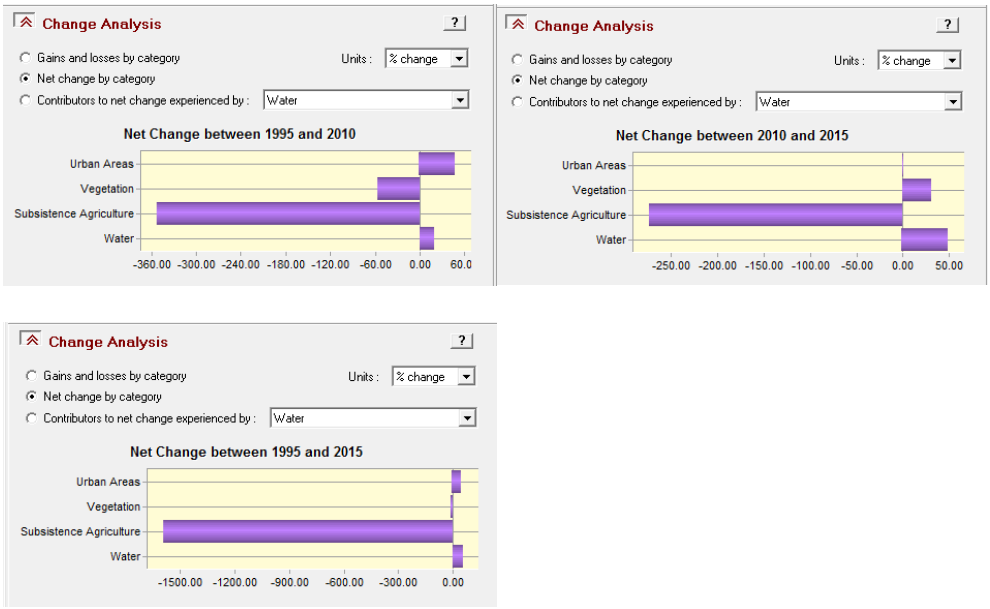

Figure 11: Percentage net change of the four LULC categories found in Kampala in terms of gains and losses.

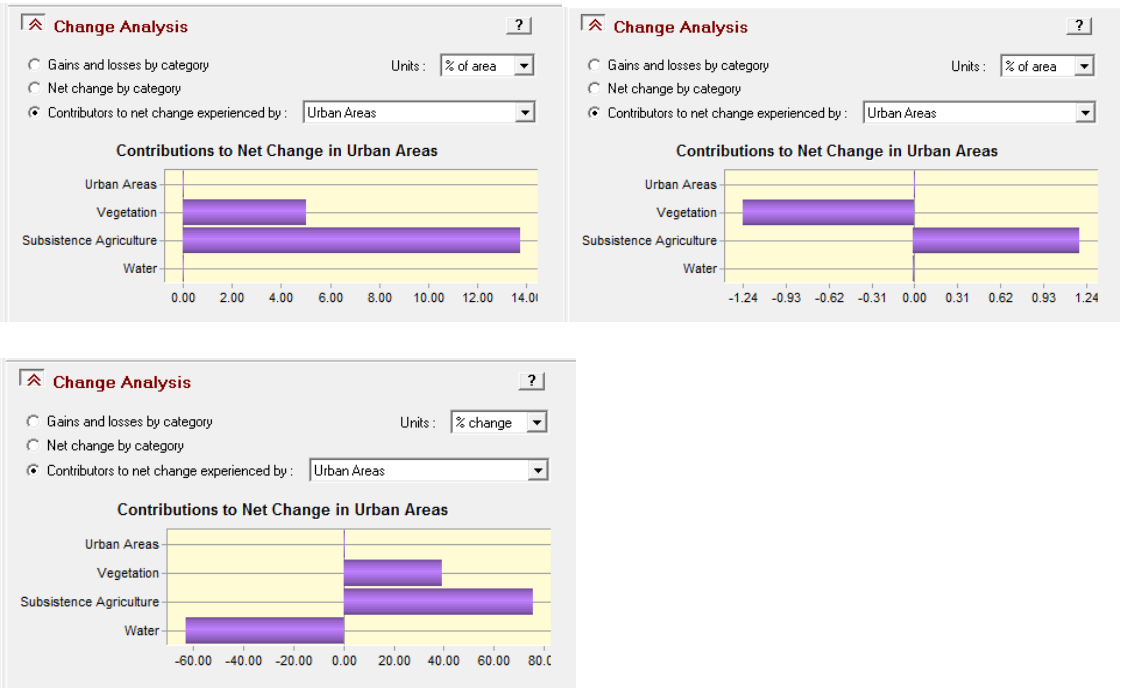

Figure 12: Major contributors to net change of urban areas.

To further evaluate the results of the LULC changes from 1995 to 2010, 2010 to 2015 and 1995 to 2015, cross- tabulation matrices (Tables 12 - 14) were developed. The diagonal entries in the Tables 12-14 highlighted in bold show the total amount of persistence of that LULC between the two time periods. The bottom row shows the quantity gained for each LULC category while the right-hand column shows the amount that has been lost. The gain for each group is obtained by subtracting the persistence from the column total while the loss is obtained by subtracting the persistence from the row total. A visual analysis of gains, losses and persistence, are shown in Figure 13, showing that urban areas have expanded towards the city boundary.

Table 12: *General cross-tabulation matrix comparing the 1995 classification map and the 2010 classification map.*

		2010					
	Category	Water	Subsistence agriculture	Vegetation	Urban areas	Total	Loss
	Water	**309**	42	42	35	428	119
	Subsistence agriculture	27	**8704**	9138	60557	78426	69722
	Vegetation	52	4534	**16595**	23609	44790	28195
	Urban areas	141	4016	2949	**72315**	79421	7106
	Total	529	17296	28524	156516	203065	
	Gain	220	8592	11929	84201		
1995							

Table 13: *General cross-tabulation matrix comparing the 2010 classification map and the 2015 classification map.*

		2015					
	Category	Water	Subsistence agriculture	Vegetation	Urban areas	Total	Loss
	Water	**432**	25	67	5	529	97
	Subsistence agriculture	216	**2325**	9183	5572	17296	14971
	Vegetation	351	1631	**16697**	9845	28524	11827
	Urban areas	61	645	14943	**140867**	156516	15649
	Total	1060	4626	40890	156289	202865	
	Gain	628	2301	24193	15422		
2010							

Table 14: *General cross-tabulation matrix comparing the 1995 classification map and the 2015 classification map.*

		2015					
	Category	Water	Subsistence agriculture	Vegetation	Urban Areas	Total	Loss
	Water	**375**	7	43	3	428	53
	Subsistence agriculture	102	**1801**	15457	61066	78426	76625
	Vegetation	309	1318	**16725**	26238	44590	27865
	Urban	274	1500	8665	**68982**	79421	10439
	Total	1060	4626	40890	156289	202865	
	Gain	685	2825	24165	87307		
1995							

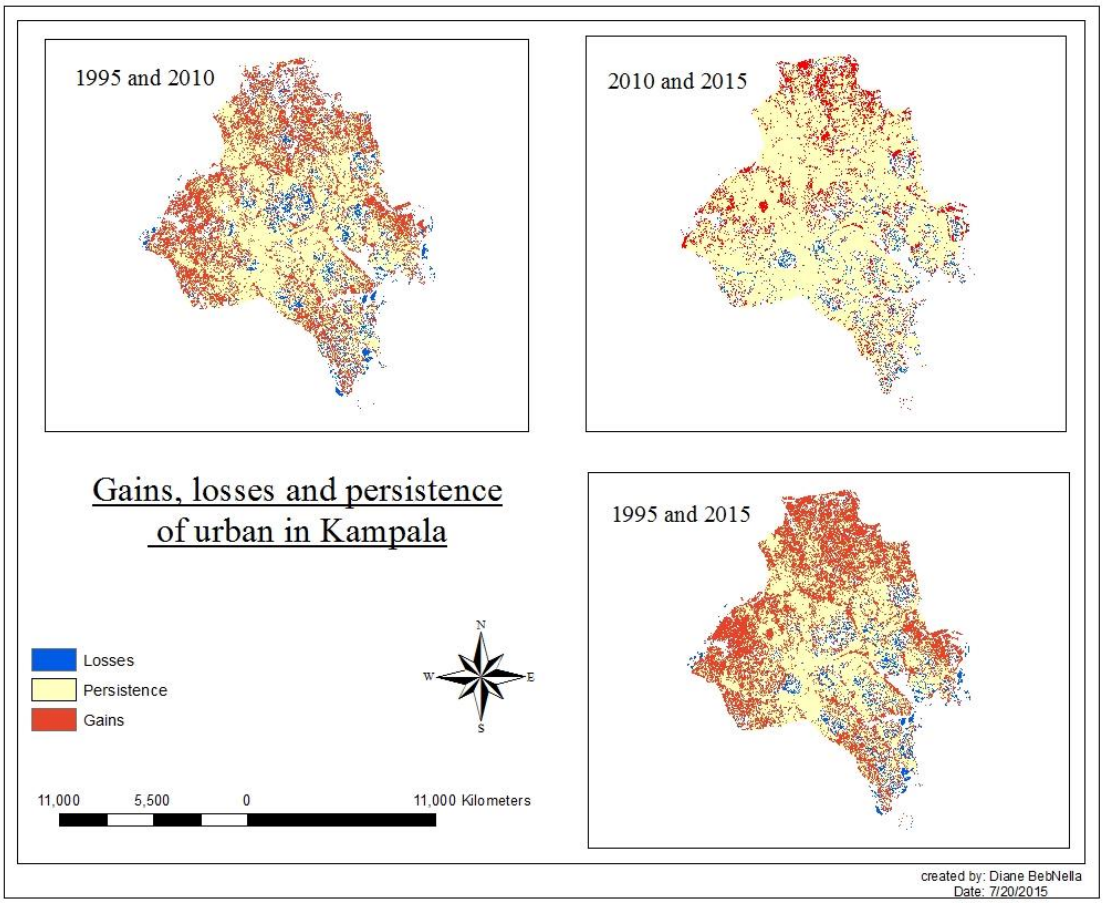

Figure 13: Gain, losses and persistence of urban areas in Kampala.

4.3 Markov Simulation

Figures 14 and 15 show the distance to road and distance to disturbance maps produced in TerrSet IDRISI. These maps served as explanatory variables for Markov Chain Simulation. The MLP achieved an accuracy rate of 85 % and a Root Mean Square Error of 0.25 for the year 2015.

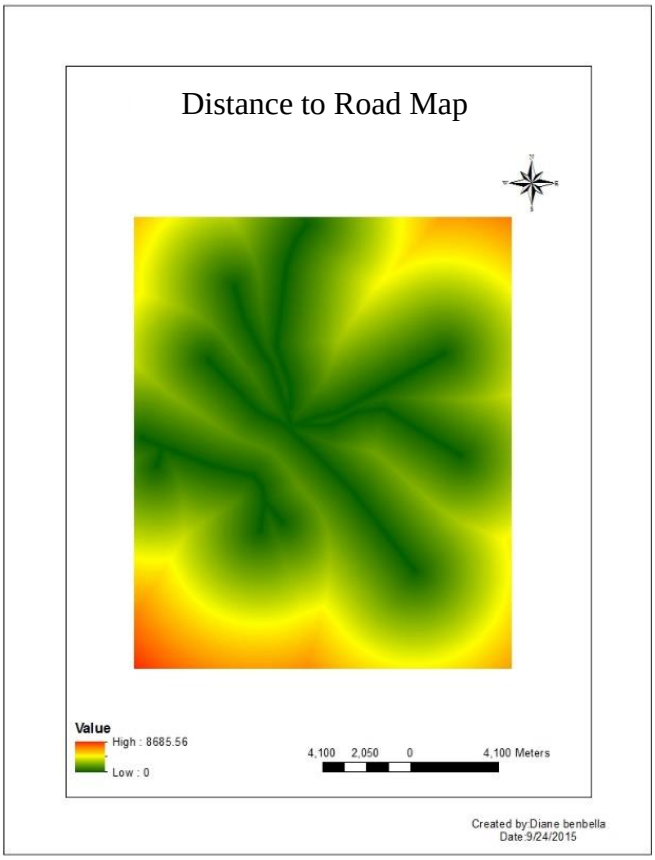

Figure 14: Distance to road map.

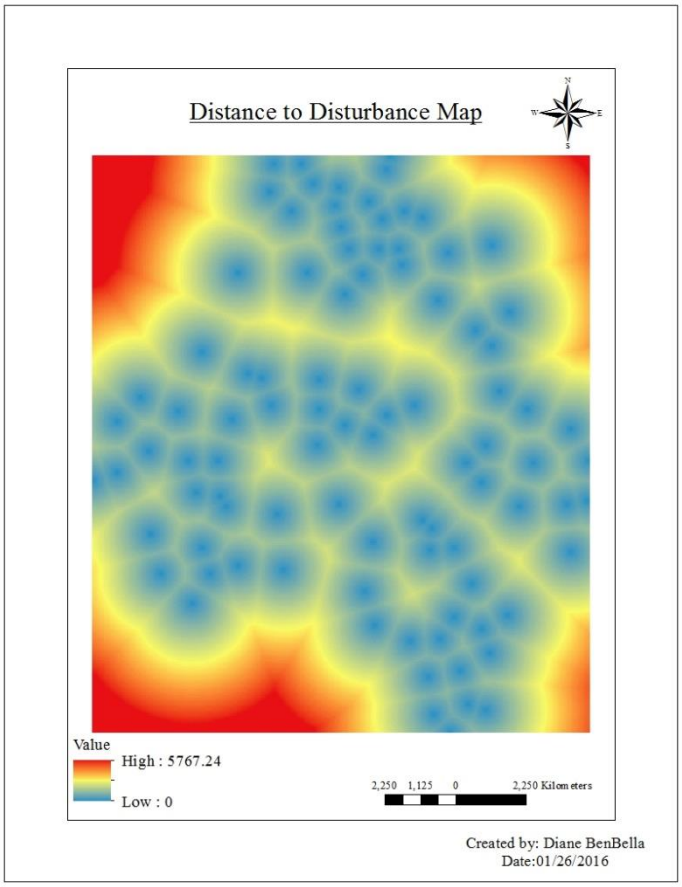

Figure 15: Distance to disturbance map.

A probability transition matrix (Table 15) was then generated to show the probability of one pixel changing to another LULC or remaining in its original LULC. This transitional matrix was essential in predicting the 2025 classification map.

Table 15: *A probability matrix that shows the probability of a given pixels changing to a different LULC category or remaining as is.*

Given	Probability of changing to			
	Water	Subsistence agriculture	Vegetation	Urban areas
Water	0.8867	0.0667	0.0465	0
Subsistence agriculture	0	0.1669	0.476	0.6855
Vegetation	0	0.1271	0.5752	0.2974
Urban areas	0	0.0451	0.0204	0.9338

Before the 2025 prediction map was obtained, the model was used to generate a 2015 prediction map based on the 1995 and 2010 classification map. This map was first visually compared to the actual 2015 classification map (Figure 16). The model was validated using the Kappa indices. The standard Kappa index ($K_{standard}$) between the simulated map and the actual map was 82 %. The Kappa for no information (K_{no}) for 2015 was 85.94 %. The Kappa for the grid-cell level location was 87.76% and, the Kappa for the stratum-level location was 87.76%. All these values are greater than 70% which proves that the Markov simulation model was well designed. Another validation method of the Markov simulation utilized in this study was the validation map (Figure 17) that was obtained directly from the Land Change Modeler. The red misses show places where the model failed to predict urban expansion. The yellow false alarms represent regions where the model tended to over predict urbanization expansion while the green hits show where the model accurately predicted urban expansion. After the accuracy of the model was met, a 2025 prediction map was obtained (Figure 18).

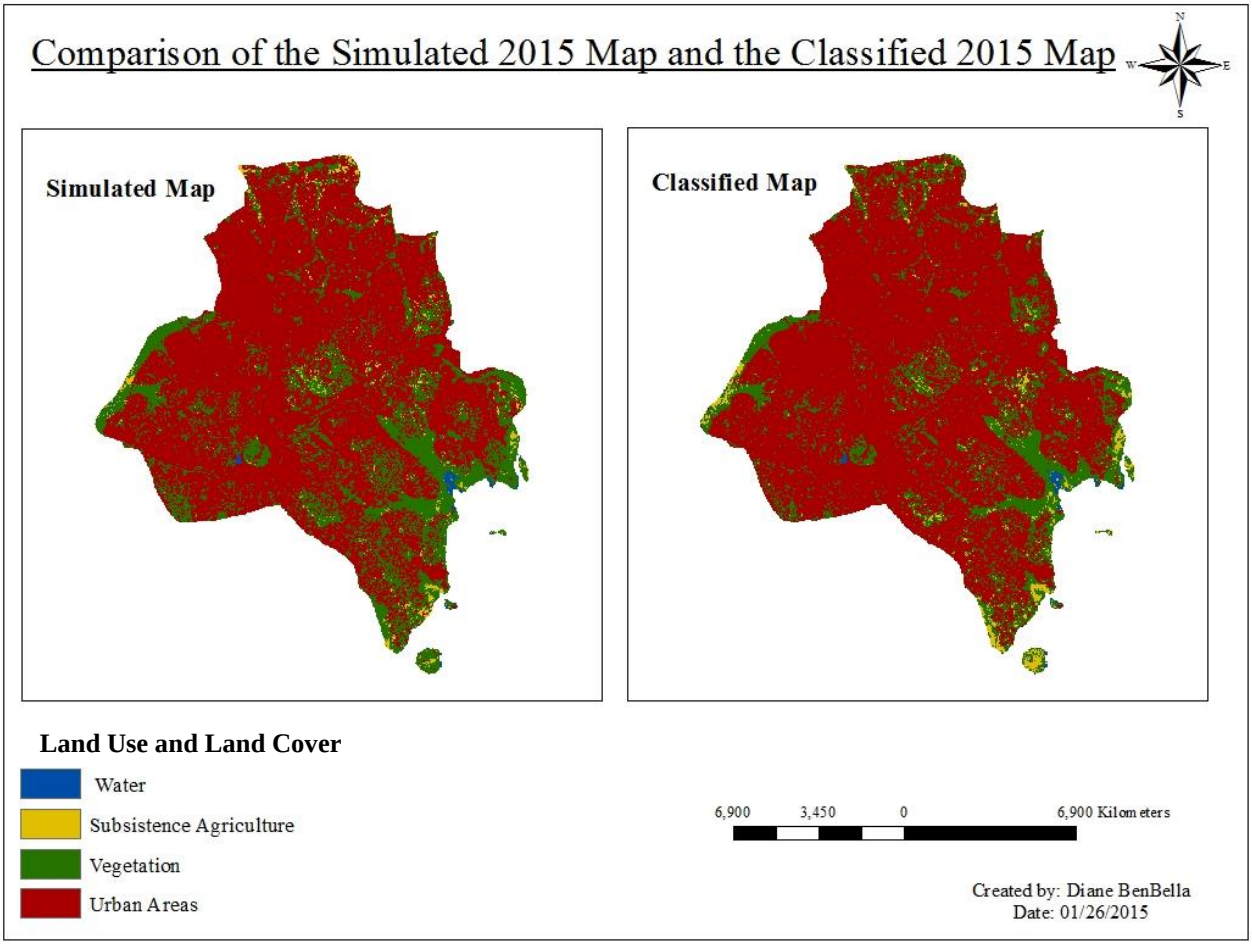

Figure 16: A visual comparison of the 2015 simulated map (left) from Markov simulation and the 2015 classified map (right).

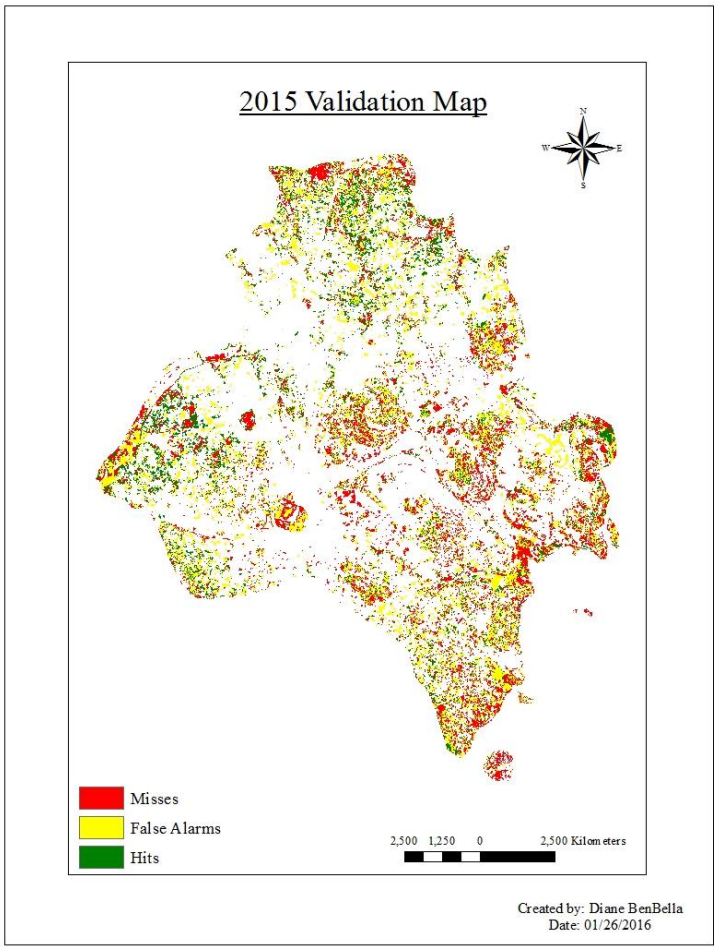

Figure 17: Validation map showing the hits, misses and false alarms of the Markov Simulation.

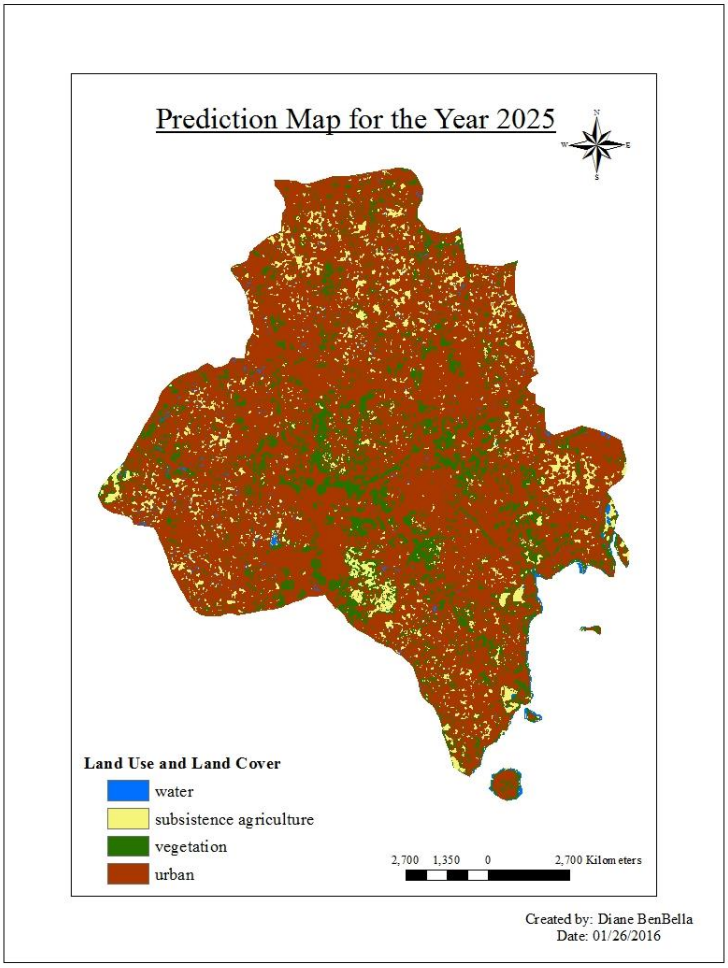

Figure 18: 2025 Prediction map of LULC types.

The 2025 map suggests that there will be significant expansion of urban areas in the western and eastern part of the district. However, the process of urbanization is a very complex and multi-faceted process. There are other non-quantifiable variables that cause urbanization such as policy and globalization that were not be analyzed in this study that could alter this prediction.

4.4 Drivers of Urbanization

4.4.1 Population growth

The population growth in Kampala has steadily increased from 1995 to 2013 (Figure 19). The population growth rate between 1995 and 2002 was about 3.9 % and about 5.1 % from 2002 to 2015 (UBOS, 2015). Currently, the population in Kampala is 1,923,700 (World Bank, 2013). This number is expected to double in the next ten years.

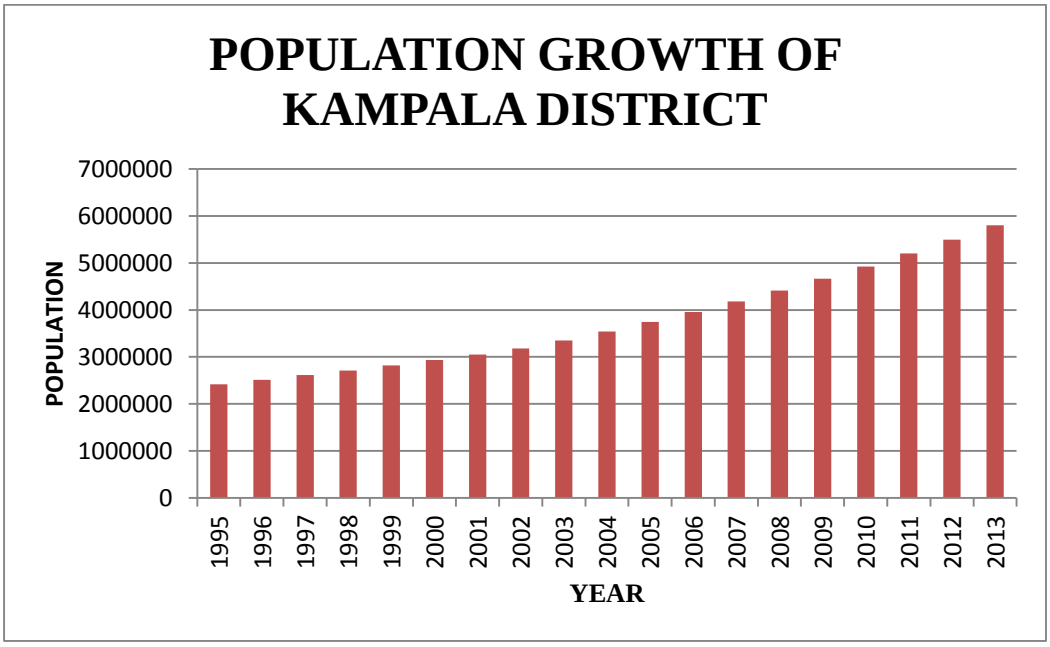

Figure 19: Population growth of Kampala from 1995 to 2013.

Figures 20 -22 below show the different population densities of the five divisions of Kampala in 1995, 2010 and 2015. In 1995, Kawempe division had the highest population of 6.1 people per square kilometer. Rubaga division had the second highest population density of 5.7 people per square kilometer. Makindye had the third highest population density of 4.7 people per square kilometer followed closely by Central division with 4.5 people per square kilometer. Nakawa had the lowest population density of 2.9 people per square kilometer. In 2010,

Kawempe division continued to have the highest population density of 12.4 people per square kilometer. This is a 50 % increase from the year 1995. Rubaga had a 51 % increase in population density in 2010 making the new population density to be 11. 5 people per square kilometer. Makindye had a population density increase 50 % bringing the population density in 2010 to 9.5 people per square kilometer. Central Division had the lowest percentage increase of 46% bringing the total population in 2010 to 8.4 people per square kilometer. Nakawa division had the highest population increase of 56 % bringing the new population density to 6.6 people per square kilometer. However, it still maintained the lowest population density of the five divisions. In 2015, Kawempe, Rubaga, Makindye Central had a 10 % population density increase bringing the new population densities to 13. 7, 12.0, 10.6 and 9.3 people per square kilometer respectively. Nakawa maintained having the highest population density increase of 16 % which brought the new population density to 8 people per square kilometer. However, like 2010, it had the lowest population of the five divisions.

The spatial distributions and patterns of population density were consistent with the distribution of urban areas found in the LULC maps of 1995, 2010 and 2015. Overall, the year 1995 had the lowest population density corresponding to the lowest percentage of urbanization. The highest increase in population density occurred between 1995 and 2010 doubling for most of the divisions. Urbanization also increased by 18.77% in this period as well. This shows that there is a positive correlation between urbanization and population density. From 2010 to 2015, there was a 4% increase in urban areas while the population density increased by 10%. Overall from 1995 to 2015, the population densities of Kawempe, Rubaga, Makindye, Central Division and Nakawa rose by 57%, 56%, 55 %, 51 % and 62 % respectively. Likewise, the percentage increase in urban areas was 35%, 30%, 20% 10% and 5% for Kawempe, Nakawa, Rubaga,

Makindye and Central division respectively for the years between 1995 and 2015. Kawempe and Nakawa divisions, the northern parts of Kampala district, had the largest increase in population density as well as the biggest increase in urbanization on the LULC map.

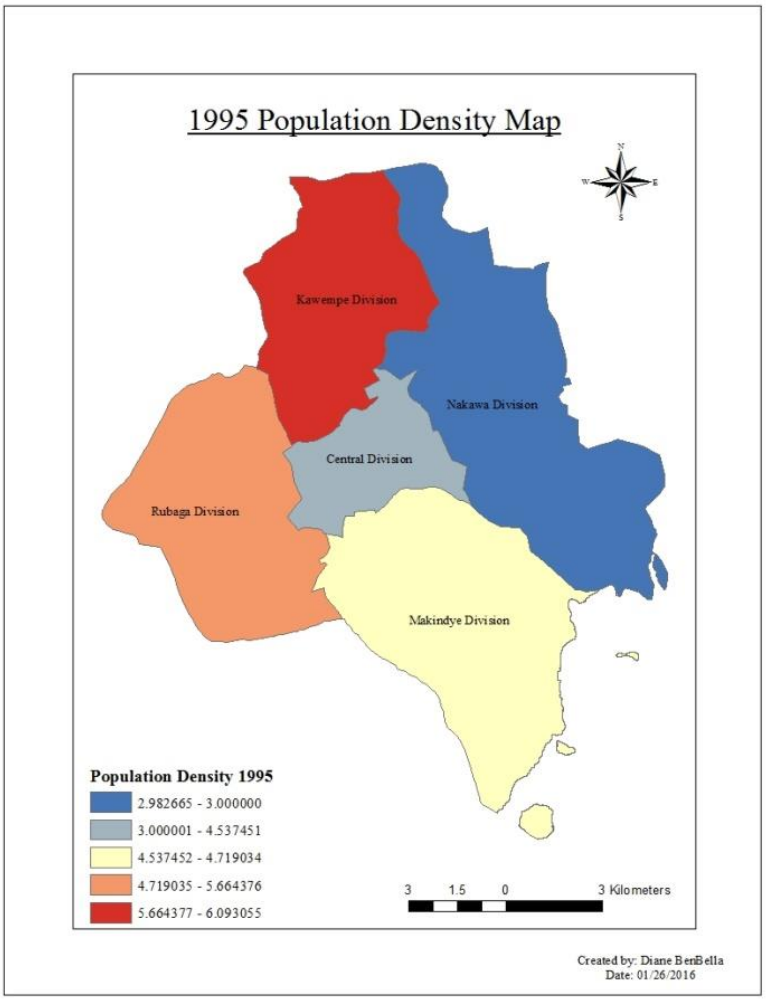

Figure 20: The population density of the five divisions of Kampala in 1995.

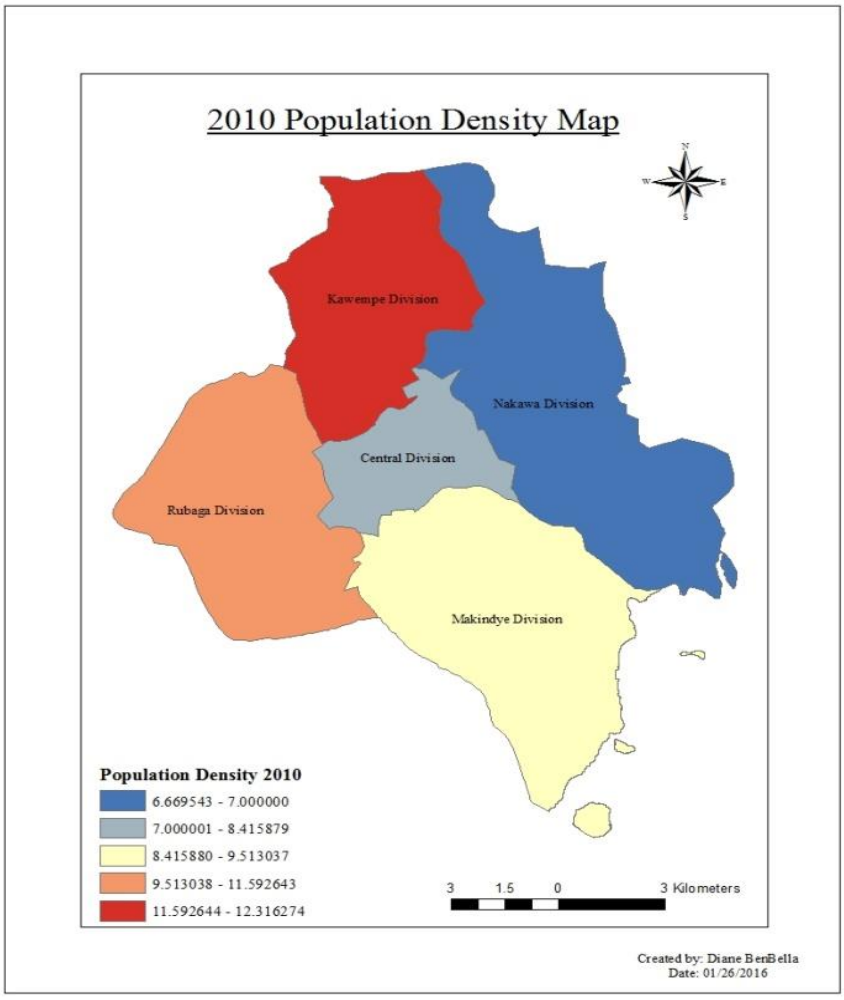

Figure 21: The population density of the five divisions of Kampala in 2010.

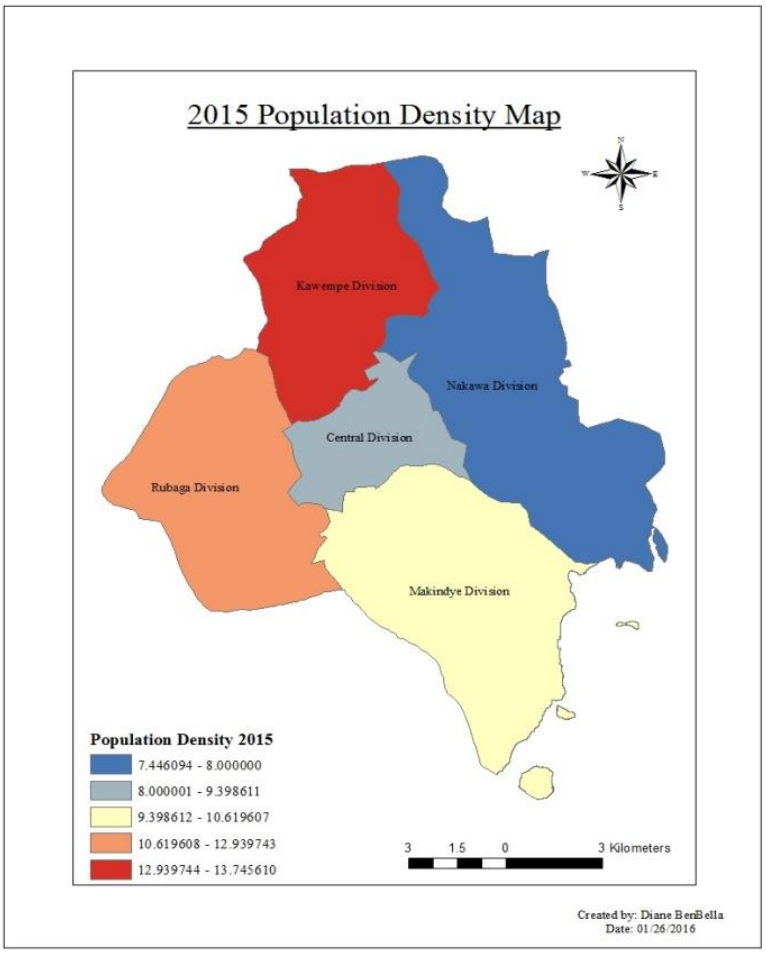

Figure 22: The population density of the five divisions of Kampala in 2015.

4.4.2 GDP Per Capita

Uganda's GDP per capita has also increased from the ear 1995 to the year 2013 (Figure 23). Figure 24 shows a graphical comparison of GDP per capita and increased urbanization. Both variables have increased over the three temporal periods. From the graph, we can deduce that there is a positive relationship between GDP per capita and increased urbanization.

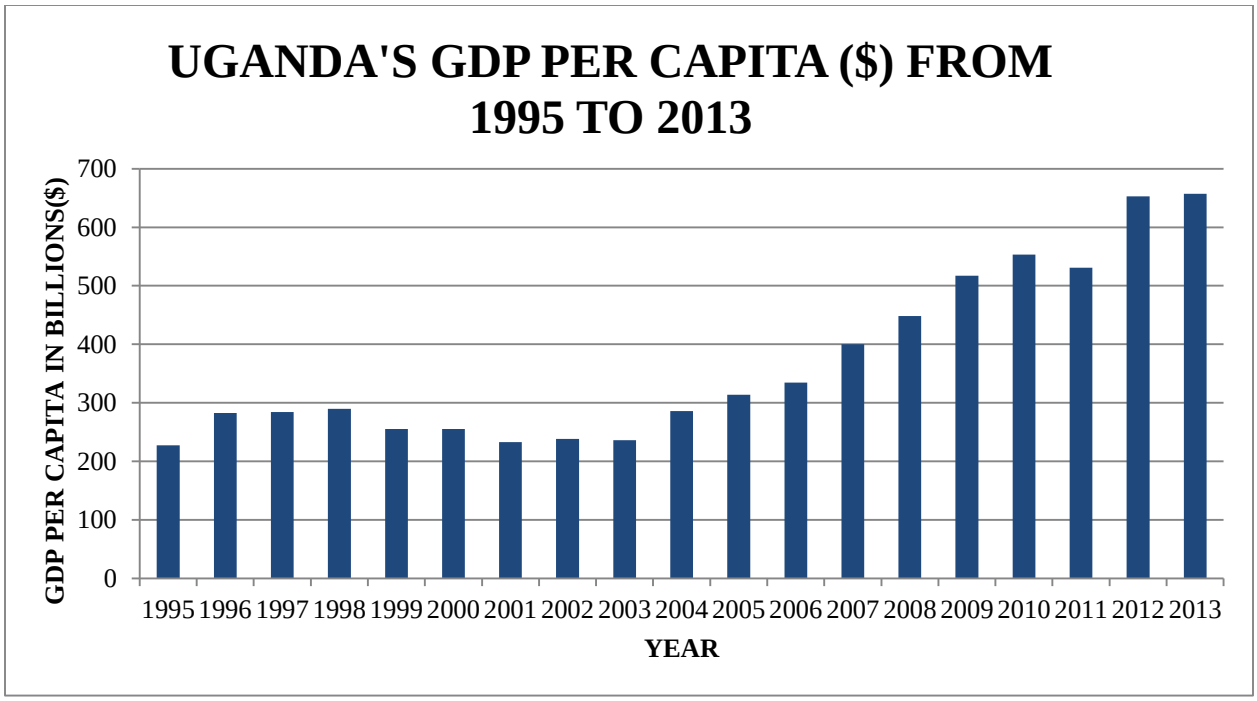

Figure 23: Uganda's GDP per Capita from 1995 to 2013 in US dollars.

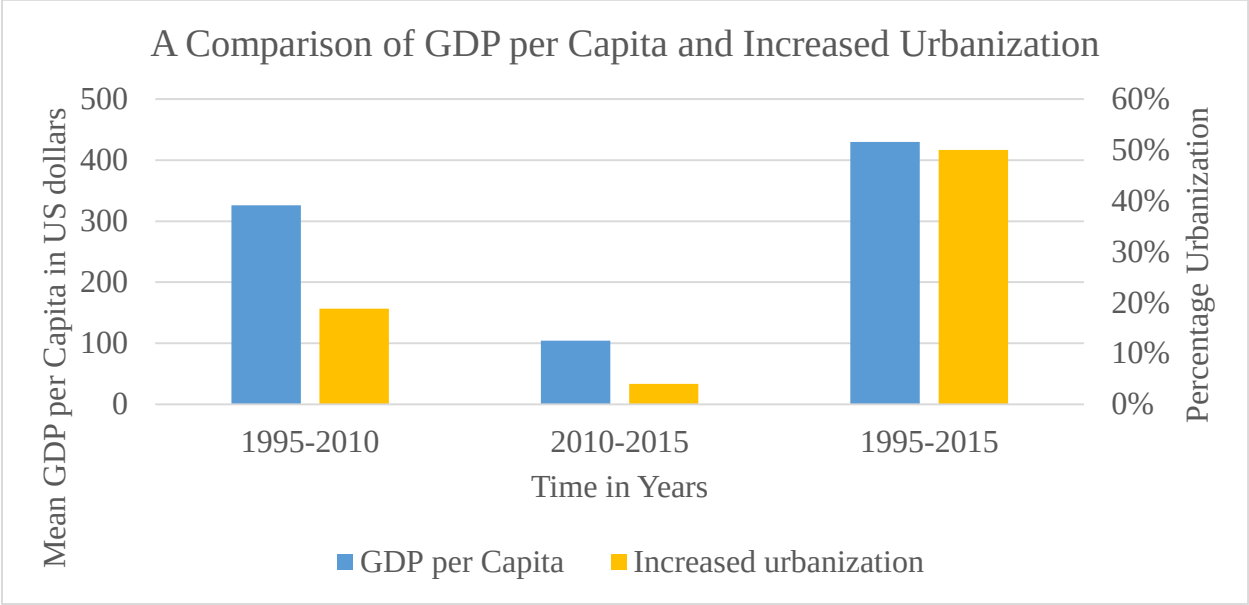

Figure 24: A graphical comparison of GDP per Capita and Increased Urbanization.

4.4.3 Foreign Direct Investments (FDI)

There has been an increment in Foreign Direct Investments (FDI) in Uganda (Figure 25) from 1995 to 2013. Figure 26 shows a graphical comparison of FDI and increased urbanization. Both variables have increased over the three temporal periods. From the graph, we can deduce that there is a positive relationship between FDI and increased urbanization.

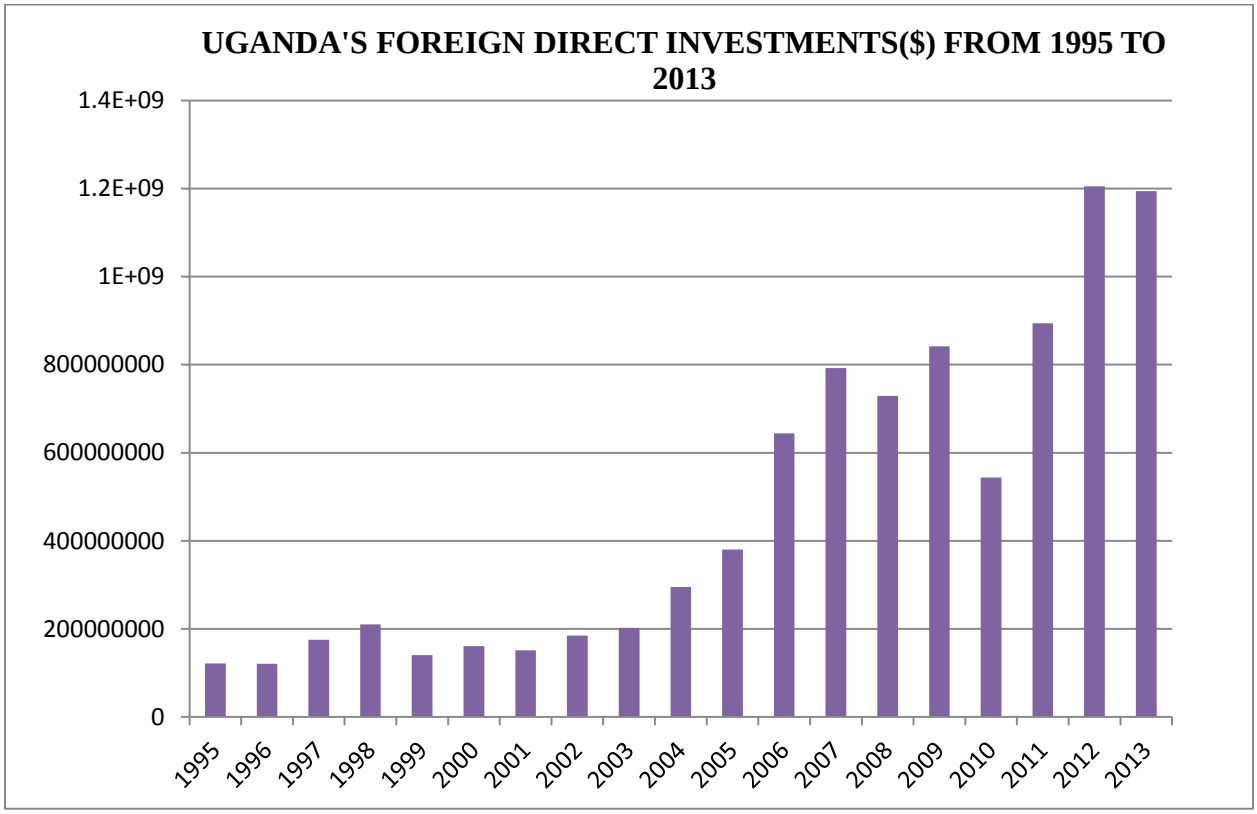

Figure 25: Uganda's FDI from 1995 to 2013 in US dollars.

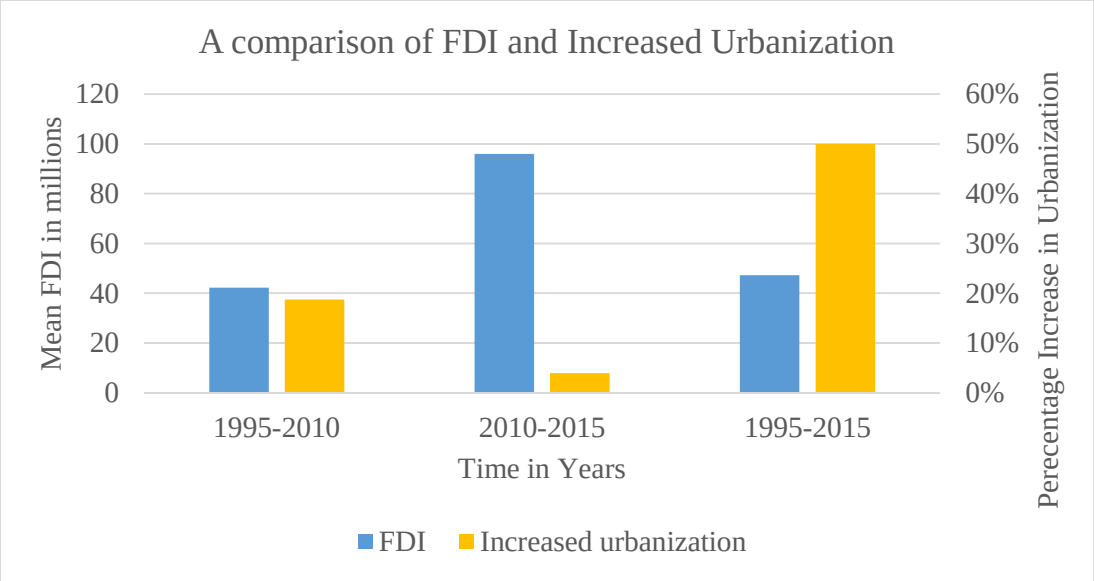

Figure 26: A graphical comparison of FDI and Increased Urbanization.

CHAPTER 5

DISCUSSION AND CONCLUSION

In this chapter, we discussed the findings from this study according to the research questions.

5.1. Spatial and Temporal Patterns of LULC change in Kampala

The first question is: *What are the spatial and temporal patterns of LULC changes in Kampala over the last 20 years and how will these patterns change over the next 10 years?*

The Landsat images were classified using ANN and SMA. ANN proved to be a more superior method because it produced classification maps that were consistent with previous studies as well as having a higher overall classification accuracy (Vermeiren et al., 2012). LULC types have significantly changed in Kampala in the last twenty years. In 1995, both urban areas and subsistence agriculture dominated the Kampala Landscape with 39% and 38.6 % of the total area. However, in 2010 and 2015, urbanization became the dominant LULC type occupying 77 % and 80 % respectively. Subsistence agriculture significantly reduced to 10% and 5 % in 2010 and 2015.Vegetation also decreased in both 2010 and 2015. Water appeared to have no significant change despite the fact that change detection analysis showed.

The spatial patterns of urbanized areas from the study showed that the developed areas in Kampala have been sprawling in all directions especially in its Northern part. Over time, Nakawa has developed into the industrial center of Kampala district and holds prominent building such as the Uganda Industrial Research Institute and Uganda Revenue Authority. As a result of increased urbanization along the edges of the city, this process has also spilled to the neighboring districts of Wakiso in the North and Mukono in the North East. These districts are fast becoming urbanized as well as heavily populated. This creates a free flow of migrants. As predicted using Markov simulation, the LULC map of 2025, urban areas will occupy 90 % of Kampala.

Subsistence farm lands will decrease to 2% while vegetated areas will drop to 10 %. Unless sustainable measures are put in place, Kampala will eventually lose its entire green environment.

5.2. LULC and Urbanization

The second research question is: *How has urbanization driven these changes of LULC types?*

Based on the results of this study, we concluded that urbanization has altered the spatial distributions and patterns of LULC types in Kampala As a result, a significant decrease in the green environment (subsistence agriculture and vegetation) has taken place in the city. Vegetation loss is a major threat to biodiversity and causes species extinction as a result of habitat fragmentation. Vegetation loss also leads to loss of ecosystem services such as the provision of rainfall and decomposition of wastes. When there is a rainfall shortage, plants are unable to get enough water to grow, this leads to drought. Drought will further drive LULC types to change from luscious green vegetation to more drought-resistant shrubs and bare land.

Also, the loss of land for subsistence agriculture is alarming because it will put food production for the increasing population at risk. This would mean depending on other districts to meet the food demands of Kampala city dwellers as well as their own demands for. Consequently this could that alter their LULC as well since forests and wetlands will be cleared in order to carry out more intensive food production so as to feed the overwhelming city population.

5.3. Factors that affect Urbanization

The third research question is: *What are the major drivers of urbanization?*

Population growth was the primary driver of LULC changes in Kampala for this study. Kampala's population has been increasing due to the high birthrate and migrations. In 1995, the total population in Uganda was approximately 725,697. Today, the population is approximately 1.6 million. Kampala has continued to be the hub of all economic, social, commercial, industrial and political activities attracting large numbers of migrants. As the population increases over time, the need for living space also increases. Consequently, subsistence agriculture fields, as well as vegetated areas, have been converted to into urban areas. Other factors that have led to increased urbanization in Kampala as determined in this study include distance to roads, distance to previous disturbance and, economic opportunities. People tend to settle along road networks because the distance to roads and the distance to previous disturbance increase their access to business opportunities, medical facilities, and schools and provide help for personal development. A healthy economy measured in GDP per capita and FDI facilitates the creation of jobs, better education systems, and scientific research attracting massive waves of migrants. Increased economic growth has also brought about constructions of big malls such as Garden City, Metroplex shopping mall, and Acacia Mall. The building of Garden City mall brought a bit of a controversy because it was built on a former wetland. Kampala's wetlands have been rapidly disappearing and are being replaced by urban structures. However, the population is still growing, and the land is not expanding. This is leading to pressure on the little available resources. Kampala is also now home to several slums such as Bwaise that are characterized by poor sanitation, flooding and substandard housing as a result of urban sprawling.

Policy has also played a significant role in urbanization. The 1998 land policy of Uganda formally recognized individuals as private owners of *mailo* land. During the era of colonization, British colonialists drafted the 1900 Buganda Agreement that divided Kampala's land into crown land and mailo land. The crown land was under their control while *mailo* land was under the supervision of the Buganda kingdom. Individuals did not have any rights to the lands and, therefore, could not manipulate the property in any way. After 1998, there was mushrooming of private houses and industries that coincidence with the 1995- 2010 temporal period that had the most amount of urbanization.

5.4. Conclusions

This study demonstrated the success of using ANN and SMA for conducting LULC classification of Kampala that is a complex landscape and dominated by mixed pixels. However, ANN in this study performed the classification better than SMA. The classification results of this research were in agreement with the work of Vermeiren et al. (2012) and the CICRED UG4 project that showed the same spatial patterns of Northern urban expansion of Kampala. The increase in urban areas, however, is at the expense of notably vegetated and subsistence agriculture lands. Population growth is the major factor that has driven the expansion of urban areas in Kampala, which is in agreement with the work of Vermeiren et al. (2012). Distance to roads, distance to disturbance, GDP and, FDI have further enhanced urbanization. The study also shows that the city is bound to lose most of its greened areas as evidenced by the 2025 prediction map unless adequate measures are put in place. These measures include making social services more accessible to the rural populations and not just the city dwellers. The Ugandan government can improve the standard of health facilities and schools in the rural areas by providing people there with the necessary facilities and attracting workers to work there with higher salaries

offered. This will decrease the migration of people from rural areas to urban areas and encourage people to migrate from urban to rural areas. Environmental bodies such as The National Environmental Authority should implement the strict policies that have been passed by parliament in a bid to protect wetlands from encroachment by people and investors. These are a few of my suggestions, but this study can be used by policymakers to implement policies that they deem fit.

5.5. Limitation of this study and future research

One of the biggest limitations of this study was its inability to use more statistically advanced methods to determine the relationship between the LULC changes and their drivers. This study also only focused on socio-economic factors and never took into account biophysical factors such as soil, climate, and geology. Future studies can accurately and exhaustively investigate the relationships between these factors and LULC changes.

REFERENCES

Ade, M.A., Afolabi, Y.D. (2013). Monitoring Urban sprawl in the federal Capital Territory of Nigeria using remote sensing and GIS techniques. Ethiopian journal of Environmental studies and Management Vol 6 No.1 2013.

Araya, Y.H.; Cabral, P. (2010). Analysis and Modeling of Urban Land Cover Change in Setúbal and Sesimbra, Portugal. *Remote Sens.***2010**, *2*, 1549-1563.

Bischof, H., Schneider, W., Pinz, A.J. (1992). Multispectral classification of Landsat-images using neural networks. IEEE Transactions on Geoscience and Remote Sensing, 30(3), pp. 482-490.

Civco, D.L. (1993). Artificial neural networks for land-cover classification and mapping. International Journal of Geographical Information Systems, 7(2), pp. 173-186.

Cohen, B. (2006). Urbanization in developing countries: Current trends, future projections, and key challenges for sustainability. Technology in society 28, no. 1 (2006): 63-80.

Dennison, P.E. and D.A. Roberts. (2003). Endmember selection for multiple endmember spectral mixture analysis using Endmember Average RMSE. Remote Sensing of Environment, 87, 123-135.

Dubovyk, Olena, Gunter Menz, Christopher Conrad, Elena Kan, Miriam Machwitz, and Asia Khamzina. (2013). Spatio-temporal analyses of cropland degradation in the irrigated lowlands of Uzbekistan using remote-sensing and logistic regression modeling. Environmental monitoring and assessment 185, no. 6 (2013): 4775-4790.

Fan, F., Weng, Q., Wang, Y. (2007). Land Use and Land Cover Change in Guangzhou, China, from 1998 to 2003, Based on Landsat TM/ETM+ Imagery. Sensors 2007,7. 1323-1342.

Gardner, M. W., and S. R. Dorling. (1998). Artificial neural networks (the multilayer perceptron)—a review of applications in the atmospheric sciences. Atmospheric environment 32.14 2627-2636.

Geymen, A., Baz, I. (2008). Monitoring urban growth and detecting land cover changes on the Istanbul metropolitan area. Environment Monitoring Assessment 136:449-459. DOI: 10.1007/S10661-007-9699-x.

Hartfield, Kyle A., Katheryn I. Landau, and Willem JD Van Leeuwen. (2011). Fusion of high resolution aerial multispectral and LiDAR data: Land cover in the context of urban mosquito habitat." Remote Sensing 3, no. 11 (2011): 2364-2383.

J. J. Settle and N. A. Drake (1993). Linear mixing and the estimation of ground cover proportions, International Journal of Remote Sensing, 14:6, 1159-1177

Jain Anil K , Mao J and Mohiuddln, (1996). Artificiale Neural Network: A tutorial.

Keller, J., and R. Lamprecht. (1995). Road dust as an indicator for air pollution transport and deposition: an application of SPOT imagery. Remote Sensing of Environment 54, no. 1 (1995): 1-12.

Keuchel, J., Nauman, S., Hweiler, M., Siegmung, A. (2003). Automatic land cover analysis for Tenerife by supervised classification using remotely sensed data. Remote sensing of Environment 86 (2003)530-541.

Lambin, E., Geist, H. (2007). Causes of Land Use Land Cover (LULC) change. Land-use & Land-cover Change and Environmental Monitoring.

Li, M., Zang, S., Zhang, B., Li, S., and Wu, C. (2014). A Review of Remote Sensing Image Classification Techniques: the Role of Spatio-contextual Information. European Journal of Remote Sensing 47 (2014): 389-411.

Li, X., Yeh, A., (2004). Analyzing spatial restructuring of land use patterns in a fast growing region using remote sensing and GIS. Landscape and planning 69 .335-354

Lillesand, Ralph W. Kiefer, and Jonathan W. Chipman. (2008). Remote Sensing and Image Interpretation, Sixth edition Thomas M., john wiley and sons, Inc. New Jersey.

Lopez,E., Bocco,G., Mendoza, M., Duhau, E. (2001). Predicting land cover and land use in the urban fringe A case in Morelia city, Mexico. Landscape and Urban planning 55 (2001)271-285.

Lu, D., and Qi. Weng. (2007). A survey of image classification methods and techniques for improving classification performance. International Journal of Remote Sensing, Vol. 28, No. 5, 10 March 2007, 823–870.

Madanian, M.A.,Soffianian, A., Fakheran,S. (2012). Monitoring Land Use/ Cover Changes Using Different Change Detection Techniques (Case Study: Falavarjan Area, Isfahan, Iran). International Conference on Applied life Sciences (ICALS2012).

Mallupattu, P K. and Reddy, R.R.S. (2013). Analysis of land use/ land cover changes using Remote sending data and GIS at an urban area, Tirupati, India. Scientific World Journal.2013 doi:10.1155/2013/268623.

Mendoza S, Javier Eduardo, and Andrés Etter R. (2002). Multitemporal analysis (1940–1996) of land cover changes in the southwestern Bogota high plain (Colombia). Landscape and urban planning 59, no. 3 (2002): 147-158.

Mubea, K. W., T. G. Ngigi, and C. N. Mundia. (2011). Assessing application of Markov chain analysis in predicting land cover change: A case study of Nakuru Municipality." Journal of Agriculture, Science and Technology 12, no. 2.

Mubea, K., and Menz, G. (2012). Monitoring Land-Use Change in Nakuru (Kenya) Using Multi-Sensor Satellite Data. DOI:10.4236/ars.2012.13008

Mundia, C. N., and M. Aniya. (2006). Dynamics of land use/cover changes and degradation of Nairobi City, Kenya." Land Degradation & Development 17, no. 1 (2006): 97-108.

Pijanowski, B., S. Pithadia, K. Alexandridis, and B. Shellito. (2005). Forecasting large-scale land use change with GIS and neural networks. International Journal of Geographic Information Science. 19 (2):197-215.

R G Pontius Jr. (2000). Quantification error versus location error in the comparison of categorical maps. Photogrammetric Engineering & Remote Sensing 66(8) p.1011-1016.

Reid, R.S., Kruska, R.L., Nyawira M., Taye, A., Wotton, S., Wilson, C. J., and Woudyalew M. (2000). Land-use and land-cover dynamics in response to changes in climatic, biological and socio-political forces: the case of southwestern Ethiopia. Landscape Ecology 15, no. 4 (2000): 339-355.

Riedmiller, Martin, and Heinrich Braun. A direct adaptive method for faster backpropagation learning: The RPROP algorithm. Neural Networks, 1993. IEEE International Conference on. IEEE, 1993.

Schoof, J. T., and S. C. Pryor. (2008). On the proper order of Markov chain model for daily precipitation occurrence in the contiguous United States." Journal of Applied Meteorology and Climatology 47, no. 9: 2477-2486.

Serpico, S.B., Bruzzone, L., Roli, F. (1996). An experimental comparison of neural and statistical non-parametric algorithms for supervised classification of remote sensing images. Pattern Recognition Letters, 17(13), pp. 1331-1341

Singh, Ashbindu. (1989). Review article digital change detection techniques using remotely-sensed data. International journal of remote sensing 10, no. 6 (1989): 989-1003.

Song, C., Woodcock, C.E., Seto, K.C., Lenney, M.P., and Scott A. M. (2001). Classification and change detection using Landsat TM data: when and how to correct atmospheric effects? Remote sensing of Environment 75, no. 2:230-244.

Vogelmann, J.E., S.M. Howard, L. Yang, C. R. Larson, B. K. Wylie, and J. N. Van Driel. (2001). Completion of the 1990 National Land Cover Data Set for the conterminous United States, Photogrammetric Engineering and Remote Sensing. 67:650-662

Weng, Q. (2002). Land use change analysis in the Zhujiang Delta of China using satellite remote sensing, GIS and stochastic modelling. Journal of environmental management 64, no. 3 (2002): 273-284.

Weng, Qihao. (2002). Land use change analysis in the Zhujiang Delta of China using satellite remote sensing, GIS and stochastic modelling." Journal of environmental management 64, no. 3: 273-284.

Wondrade, N., Dick, O.B., Tveite, H. (2014). GIS based mapping of land cover changes utilizing multi-temporal remotely sensed image data in Lake Hawassa Watershed, Ethiopia Environment Monitoring Assessment. DOI: 10.1007/s10661-0133491-X.

Wu, Q., Li, H., Wang, R., Paulussen, J., He, Y., Wang, m., Wang, B., Wang, Z. (2006). Monitoring and predicting land use change in Beijing using remotes sensing and GIS. Landscape and Urban Planning 78 (2006) 322-33

Xiao, J., Shen, Y., Ge, J., Tateishi, R., Tang, C., Liang, Y., Huang, Z. (2006). Evaluating urban expansion and land use change in Shijiazhuang, China, by using GIS and Remote Sensing. Elsevier. Doi:10.1016/j. landurbplan 2004.12.005.

Yuanbin, C., Zhang, H., Wenbin, P., Chen, Y., and Wang, X. (2012). Urban Expansion and Its Influencing Factors in Natural Wetland Distribution Area in Fuzhou City, China. Chinese Geographical Science 22, no. 5 (2012): 568-577.

VITA

Graduate School
Southern Illinois University

Diane Esaete Benbella

dianebenbella@gmail.com

Makerere University, Kampala, Uganda

Bachelors of Science in Conservation Biology (Honors), January 2012

Thesis Title:
An Evaluation and Analysis of Urban Expansion of Kampala from 1995 To 2015

Major Professor: Dr. Guangxing Wang